Article

Local immune response to food antigens drives meal-induced abdominal pain

https://doi.org/10.1038/s41586-020-03118-2

Received: 18 March 2020

Accepted: 27 November 2020

Published online: 13 January 2021

Check for updates

Javier Aguilera-Lizarraga[1,22], Morgane V. Florens[1,22], Maria Francesca Viola[1], Piyush Jain[1], Lisse Decraecker[1], Iris Appeltans[1], Maria Cuende-Estevez[1], Naomi Fabre[1], Kim Van Beek[1], Eluisa Perna[1], Dafne Balemans[1], Nathalie Stakenborg[1], Stavroula Theofanous[1], Goele Bosmans[1], Stéphanie U. Mondelaers[1], Gianluca Matteoli[2], Sales Ibiza Martínez[2,20], Cintya Lopez-Lopez[3], Josue Jaramillo-Polanco[3], Karel Talavera[4], Yeranddy A. Alpizar[5], Thorsten B. Feyerabend[6], Hans-Reimer Rodewald[6], Ricard Farre[7], Frank A. Redegeld[8], Jiyeon Si[9,10], Jeroen Raes[9,10], Christine Breynaert[11], Rik Schrijvers[11], Cédric Bosteels[12,13], Bart N. Lambrecht[12,13,14], Scott D. Boyd[15,16], Ramona A. Hoh[15], Deirdre Cabooter[17], Maxim Nelis[17], Patrick Augustijns[17], Sven Hendrix[18,21], Jessica Strid[19], Raf Bisschops[1], David E. Reed[3], Stephen J. Vanner[3], Alexandre Denadai-Souza[1,23], Mira M. Wouters[1,23] & Guy E. Boeckxstaens[1,23]✉

Up to 20% of people worldwide develop gastrointestinal symptoms following a meal[1], leading to decreased quality of life, substantial morbidity and high medical costs. Although the interest of both the scientific and lay communities in this issue has increased markedly in recent years, with the worldwide introduction of gluten-free and other diets, the underlying mechanisms of food-induced abdominal complaints remain largely unknown. Here we show that a bacterial infection and bacterial toxins can trigger an immune response that leads to the production of dietary-antigen-specific IgE antibodies in mice, which are limited to the intestine. Following subsequent oral ingestion of the respective dietary antigen, an IgE- and mast-cell-dependent mechanism induced increased visceral pain. This aberrant pain signalling resulted from histamine receptor H_1-mediated sensitization of visceral afferents. Moreover, injection of food antigens (gluten, wheat, soy and milk) into the rectosigmoid mucosa of patients with irritable bowel syndrome induced local oedema and mast cell activation. Our results identify and characterize a peripheral mechanism that underlies food-induced abdominal pain, thereby creating new possibilities for the treatment of irritable bowel syndrome and related abdominal pain disorders.

The mucosal immune system provides a balanced response to pathogens and harmless commensal bacteria or food antigens, thereby limiting unnecessary inflammation and concomitant tissue damage[2]. This is achieved by oral tolerance—the active suppression of cellular and humoral responses to orally administered antigens[3]. Viral and bacterial infections can, however, interfere with tolerance to dietary antigens, thereby perturbing intestinal homeostasis[4]. Infectious gastroenteritis is a significant risk factor for later developing irritable bowel syndrome (IBS), which is defined as a constellation of abdominal pain and altered bowel patterns. Between 3 and 36% of enteric infections lead to new-onset IBS[5], and up to 17% of patients with IBS report that their symptoms started upon gastrointestinal infection[6]. More than 10% of the general population experience symptoms of IBS, which are often triggered by food ingestion[7]. Aberrant pain

[1]Laboratory for Intestinal Neuroimmune Interactions, Translational Research Center for Gastrointestinal Disorders, KU Leuven Department of Chronic Diseases, Metabolism and Ageing, Leuven, Belgium. [2]Laboratory for Mucosal Immunology, Translational Research Center for Gastrointestinal Disorders, KU Leuven Department of Chronic Diseases, Metabolism and Ageing, Leuven, Belgium. [3]Gastrointestinal Diseases Research Unit, Queen's University, Kingston, Ontario, Canada. [4]Laboratory for Ion Channel Research, VIB Center for Brain and Disease Research, KU Leuven Department of Cellular and Molecular Medicine, Leuven, Belgium. [5]Neuroscience Research group, BIOMED, Hasselt University, Hasselt, Belgium. [6]Division of Cellular Immunology, German Cancer Research Center, Heidelberg, Germany. [7]Mucosal Permeability Lab, Translational Research Center for Gastrointestinal Disorders, KU Leuven Department of Chronic Diseases, Metabolism and Ageing, Leuven, Belgium. [8]Division of Pharmacology, Utrecht Institute for Pharmaceutical Sciences, Faculty of Science, Utrecht University, Utrecht, the Netherlands. [9]KU Leuven Laboratory of Molecular Bacteriology, Department of Microbiology and Immunology, Rega Institute, Leuven, Belgium. [10]VIB KU Leuven Center for Microbiology, Leuven, Belgium. [11]Allergy and Clinical Immunology Research Group, KU Leuven Department of Microbiology, Immunology and Transplantation, Leuven, Belgium. [12]Laboratory of Immunoregulation, VIB Center for Inflammation Research, Ghent, Belgium. [13]Department of Internal Medicine and Pediatrics, Ghent University, Ghent, Belgium. [14]Department of Pulmonary Medicine, Erasmus University Medical Center Rotterdam, Rotterdam, The Netherlands. [15]Department of Pathology, Stanford University School of Medicine, Stanford, CA, USA. [16]Sean N. Parker Center for Allergy and Asthma Research, Stanford University School of Medicine, Stanford, CA, USA. [17]KU Leuven Department of Pharmaceutical and Pharmacological Sciences, Leuven, Belgium. [18]Department of Morphology, Biomedical Research Institute, Hasselt University, Hasselt, Belgium. [19]Department of Immunology and Inflammation, Imperial College London, London, UK. [20]Present address: Laboratory of Cell Biology and Histology, Department of Veterinary Sciences, University of Antwerp, Wilrijk, Belgium. [21]Present address: Medical School Hamburg, Hamburg, Germany. [22]These authors contributed equally: Javier Aguilera-Lizarraga, Morgane V. Florens. [23]These authors jointly supervised this work: Alexandre Denadai-Souza, Mira M. Wouters, Guy E. Boeckxstaens. ✉e-mail: guy.boeckxstaens@kuleuven.be

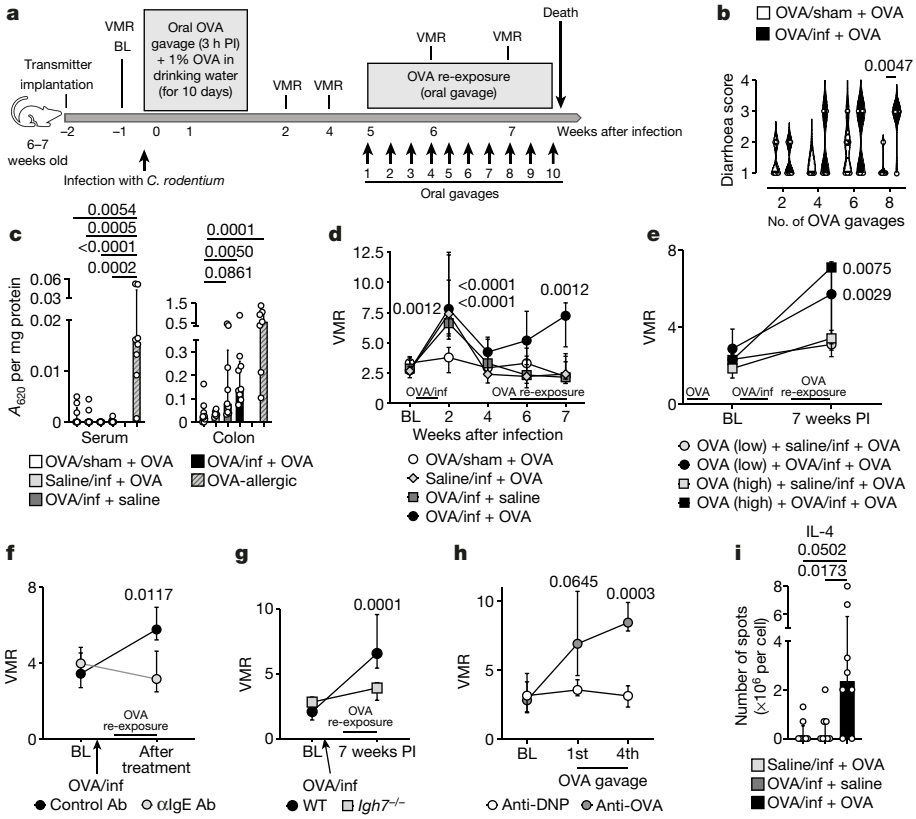

Fig. 1 | OVA-specific immune response and VHS in post-infectious mice. **a**, Experimental protocol. BL, baseline; VMR, visceromotor response. **b**, Diarrhoea scores in OVA/sham + OVA and OVA/infected + OVA mice ($n = 6$ and 8, respectively) after OVA gavages. inf, infected. **c**, Quantification of OVA-specific IgE in serum (left) and colon homogenates (right) of OVA/sham + OVA, saline/infected + OVA, OVA/infected + saline, OVA/infected + OVA and OVA-allergic mice (serum, $n = 9, 10, 10, 9$ and 8 and colon, $n = 9, 6, 9, 9$ and 7, respectively). **d**–**h**, VMR to colorectal distention (measured as area under the curve (AUC); % × ml (see Methods)) in OVA/sham + OVA, OVA/infected + saline, saline/infected + OVA and OVA/infected + OVA mice (**d**; $n = 12, 11, 11$ and 13, respectively); OVA-tolerized (high dose) + saline/infected + OVA, OVA-tolerized (high dose) + OVA/infected + OVA, OVA-tolerized (low dose) + saline/infected + OVA and OVA-tolerized (low dose) + OVA/infected + OVA mice (**e**; $n = 6, 9, 6$ and 8, respectively); OVA/infected + OVA mice treated with anti-IgE antibody or control antibody (**f**; $n = 8$ per group); OVA/infected + OVA mice with wild-type or *Igh7*$^{-/-}$ background (**g**; $n = 10$ per group); and naive mice treated with monoclonal OVA-specific IgE antibody or monoclonal anti-dinitrophenyl (DNP) antibody ($n = 7$ and 6, respectively). **i**, IL-4-producing cells in colon-draining lymph nodes from saline/infected + OVA, OVA/infected + saline and OVA/infected + OVA mice ($n = 8$ per group). *P* values shown in plots. **b**, Two-tailed Mann–Whitney test; **c**, **i**, Kruskal–Wallis test with Dunn's multiple comparisons test; **d**–**h**, two-way repeated ANOVA with Sidak's multiple comparisons test. **b**, Violin plots; **c**–**i**, median ± interquartile range (IQR).

signalling or visceral hypersensitivity (VHS) is a hallmark symptom of IBS. An increase in the number of mast cells and release of mast cell mediators have been proposed to underlie VHS[8], although the stimuli responsible for the activation of mast cells in IBS, especially in response to food intake, remain unclear. IBS is a debilitating and difficult-to-treat condition for which no curative therapies are currently available.

We hypothesized that a breakdown of oral tolerance to food antigens caused by a bacterial infection underlies food-induced VHS. We infected BALB/c mice with *Citrobacter rodentium* while exposing them to ovalbumin (OVA) in the drinking water (OVA/infected; Fig. 1a). After clearance of the infection[9], repeated oral gavages of OVA led to the development of diarrhoea, increased faecal water content and reduced transit time (Fig. 1b, Extended Data Fig. 1a, b) in infected (OVA/infected + OVA) but not in uninfected (OVA/sham + OVA) mice. We detected OVA-specific IgE antibodies in the colons of OVA/infected mice (the site colonized by *C. rodentium*) but not in the small intestine or serum (Fig. 1c, Extended Data Fig. 1c). Moreover, these mice did not show ear swelling after intradermal injection of OVA, in contrast to mice that were allergic to OVA (Extended Data Fig. 1d), suggesting a local rather than a systemic immune response.

To understand the functional implications of this altered immune reaction to a food antigen, we investigated whether re-exposure to OVA could affect pain perception. As previously described[10], mice infected with *C. rodentium* developed a transient period of increased pain response to colorectal distension, referred to as VHS, which returned to baseline after four weeks. Notably, re-exposure to OVA five weeks or more after infection resulted in VHS in OVA/infected mice but not in uninfected mice (Fig. 1d, Extended Data Fig. 1e, f), which persisted for at least four weeks after the last OVA gavage (Extended Data Fig. 1g). VHS was associated with increased mucosal permeability to sodium fluorescein (Extended Data Fig. 1h), consistent with data obtained from patients with IBS[11]. Similar findings were obtained in mice that had been tolerized to OVA before infection, indicating that an infection with *C. rodentium* can induce a breakdown of oral tolerance once established (Fig. 1e, Extended Data Fig. 1i, j). Moreover, the development of VHS was antigen-specific, as repeated gavages of bovine serum albumin (BSA) failed to affect pain perception in OVA/infected mice (Extended Data Fig. 1k, l). No differences in the relationship between intra-abdominal volume and intra-abdominal pressure (that is, compliance) were found between groups (Extended Data Table 1), excluding the possibility that inflammatory-mediated changes in wall stiffness had developed and altered nociceptive signalling.

To further investigate the role of the antigen-specific immune response to OVA in VHS, we treated mice with a monoclonal anti-IgE

antibody (Extended Data Fig. 1m). This treatment prevented the development of VHS and the increase in colonic permeability upon re-exposure to OVA (Fig. 1f, Extended Data Fig. 1n, o). We confirmed these results in IgE-deficient (*Igh7*$^{-/-}$) mice (Fig. 1g, Extended Data Fig. 1p, q). Conversely, sensitization of naive mice with the monoclonal OVA-specific IgE antibody resulted in the development of VHS upon repeated OVA administration (Fig. 1h, Extended Data Fig. 1r, s). Notably, the number of lymphocytes producing IL-4, a cytokine required for the production of allergen-specific IgE by B cells[12], was increased in colonic draining mesenteric lymph nodes of VHS mice (Fig. 1i). Together, these data indicate that a gastrointestinal bacterial infection can break oral tolerance to a dietary antigen and result in an adaptive immune response towards food antigens, leading to increased permeability and abnormal pain signalling upon re-exposure to the antigen.

As changes in the gut microbial composition have been associated with IBS[13], we investigated whether a similar phenomenon was involved in our mouse model. Exposure to OVA during *C. rodentium* infection shifted the community structure of the intestinal microbiome, compared to saline exposure, ten days after infection and after re-exposure to OVA (Extended Data Fig. 2a). Although *Robinsoniella* and *Eisenbergiella* were two of the strongest drivers of this separation, we found no significant correlations between changes in these or other genera and the development of VHS (Extended Data Fig. 2b–d). Furthermore, both antibiotic-treated (to deplete the gut microbiota) and vehicle-treated OVA/infected + OVA mice developed VHS similarly (Extended Data Fig. 2e–g). Despite the shift in microbiota composition observed in VHS mice, we show that the development of VHS is likely to be independent from the gut microbiota.

'Low-grade' inflammation and increased mast cell activation have also been proposed as underlying mechanisms of IBS, especially in post-infectious IBS[5]. Although there was mild colonic inflammation during the acute infectious phase in our mice (10–14 days after infection[10]), this was resolved in VHS or normosensitive infected mice after seven weeks (Fig. 2a, Extended Data Fig. 3a–q). Notably, however, expression of the mast-cell-restricted tryptase α/β-1 gene (*Tpsab1*) was upregulated in the colons of OVA/infected mice regardless of whether they were re-exposed to OVA (Fig. 2a), suggesting that mast cells are sensitized or activated as a result of the exposure to the dietary antigen during infection. This idea was confirmed by the finding of increased mast cell degranulation and increased release of histamine (one of the main mast cell mediators) in response to incubation with OVA-peptide 323–339 of mast cells from OVA/infected + OVA mice but not from other groups (Fig. 2b, c, Extended Data Fig. 4a–e). Notably, treatment with the mast cell stabilizer doxantrazole and genetic ablation of mast cells normalized and prevented, respectively, VHS and decreased colonic permeability (Fig. 2d, e, Extended Data Fig. 4f–j). Furthermore, elimination of B cells and plasma cells (Extended Data Fig. 4k–m) reduced levels of OVA-specific IgE and prevented the development of VHS (Fig. 2f, Extended Data Fig. 4n, o). This indicates that OVA-specific antibodies produced locally by B cells and plasma cells sensitize mast cells and subsequently mediate mast cell activation upon re-exposure to OVA.

Both histamine and biopsy supernatants from patients with IBS not only activate but also sensitize visceral afferents and dorsal root ganglia (DRG) neurons[8,14]. Mechanical stimulation of colonic splanchnic nerves, which transmit visceral pain signals to the spinal cord[15], evoked higher action potential discharge in VHS mice than in normosensitive mice (Fig. 3a), indicating that the visceral nerves of VHS mice are more sensitive. Moreover, colonic supernatant from VHS mice increased neuronal excitability compared to supernatant from normosensitive mice (Fig. 3b), and increased the sensitivity of DRG neurons to capsaicin, a specific agonist of the transient receptor potential channel TRPV1, similar to incubation with histamine (Fig. 3c, Extended Data Fig. 5a). This cation channel on nociceptors is involved in VHS in patients with IBS[14]. Incubation of DRG neurons with VHS colonic supernatant in the presence of the histamine-1 receptor (H_1R) antagonist pyrilamine

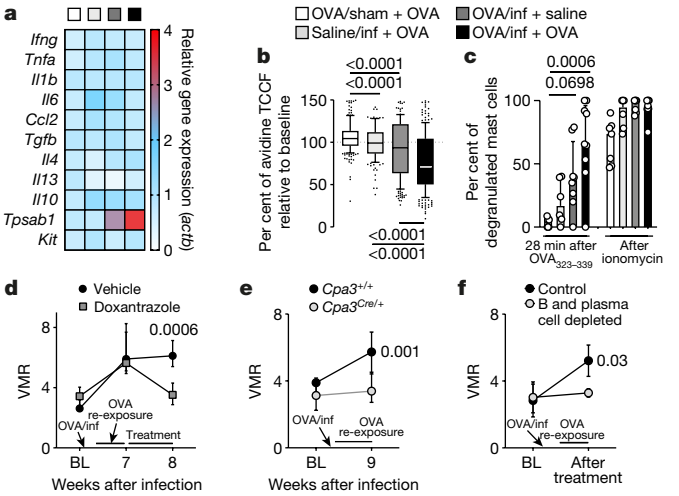

Fig. 2 | Mast cells have a key role in the development of OVA-induced VHS. **a**, Relative gene expression in colon samples from (left to right) OVA/sham + OVA, saline/infected + OVA, OVA/infected + saline and OVA/infected + OVA mice (n = 21, 11, 11 and 21, respectively, except for *Tpsab1*: n = 7, 5, 7 and 8; and *Il13*: n = 7, 9, 7 and 8)). **b**, **c**, Mast cell degranulation in OVA/sham + OVA, saline/infected + OVA, OVA/infected + saline and OVA/infected + OVA mice measured as percentage of avidin fluorescence intensity (TCCF) relative to baseline time (28 min after administration of $OVA_{323–339}$ peptide) (**b**, n = 222 cells (7 mice), 145 (6), 202 (8) and 239 (9), respectively) and percentage of total degranulated mast cells (**c**). **d**–**f**, VMR to colorectal distention (measured as area under the curve (AUC); % × ml) in OVA/infected + OVA mice treated with doxantrazole or vehicle (**d**, n = 14 and 11, respectively); mice with *Cpa3*$^{Cre/+}$ background or wild-type littermates (**e**, n = 13 and 10, respectively); and mice treated with anti-CD20 antibody and bortezomib or control antibody and vehicle (**f**, n = 3 and 4, respectively). P values shown in plots. **a**, One-way ANOVA with Sidak's multiple comparisons test; **b**, **c**, Kruskal–Wallis test with Sidak's multiple comparisons test; **d**–**f**, two-way repeated ANOVA with Sidak's multiple comparisons test. Box plots (**b**): centre line, median; box, 25th–75th percentiles; whiskers, 10th–90th percentiles; dots, outliers); **c**–**f**, median ± IQR. In **a**, *Tpsab1* expression was significantly different in OVA/infected + saline and OVA/infected + OVA mice compared with OVA/sham + OVA mice (adjusted P = 0.0173 and 0.0014, respectively).

prevented the increased excitability and TRPV1-mediated response (Fig. 3d, e), similar to our findings in patients with IBS[14]. Furthermore, treatment with pyrilamine reduced the pain response to colorectal distention in VHS mice (Fig. 3f, Extended Data Fig. 5b). These findings were confirmed in *Hrh1*$^{-/-}$ mice (Fig. 3g, Extended Data Fig. 5c), indicating that the mast-cell-mediated increase in visceral pain signalling is mediated by H_1R and involves sensitization of TRPV1 and, probably, other voltage-gated ion channels in sensory neurons.

In the upper airways, superantigens (SAgs)—microbial antigens known to cause non-specific activation of T cells—have been implicated in the pathogenesis of asthma and atopic rhinitis[16] via a bystander T helper type 2 cell (Th2)-polarized immune response against innocent antigens[17]. We reasoned that intestinal exposure to SAgs, for instance after swallowing SAgs during an episode of acute rhinitis or produced by the microbiome, could trigger a similar immune response to dietary antigens as we observed with bacterial gastroenteritis. Similar to OVA/infected mice, mice that were exposed to OVA in the presence of staphylococcal enterotoxin B (SEB) developed VHS when re-exposed to OVA (even if they had been tolerized to OVA before SEB administration), and displayed increased mucosal permeability compared to saline/SEB mice (Extended Data Fig. 6a-c). In SEB-VHS mice, *Tpsab1*, *Il4*, *Il6* and *Il10* were upregulated (Extended Data Fig. 6d). Mast cell activation mediated these changes, as they were blocked by doxantrazole and were absent in *Cpa3*$^{Cre/+}$ mice (Extended Data Fig. 6e–h). Colonic OVA-specific IgE was higher in SEB-VHS mice than in saline/SEB mice

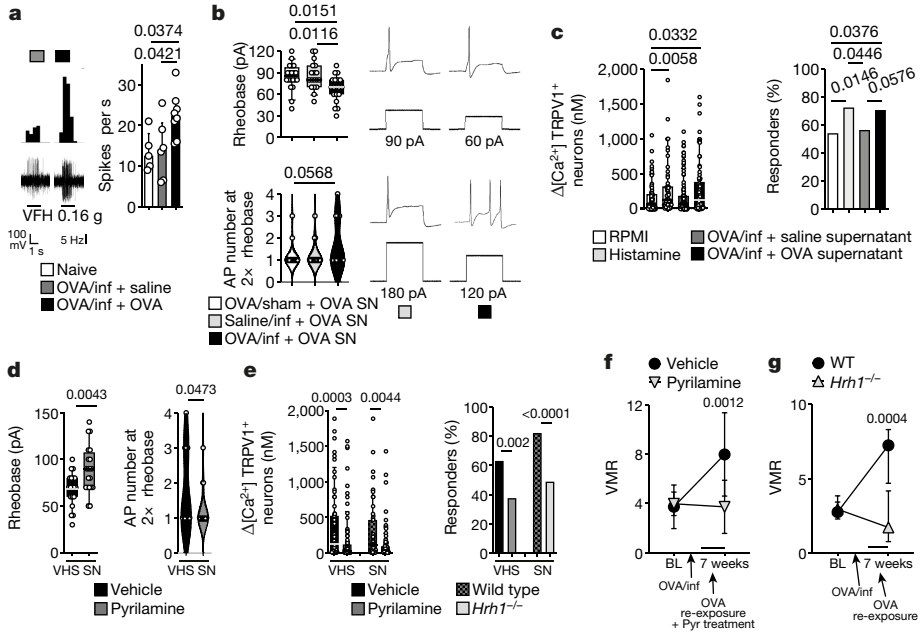

Fig. 3 | H_1R-mediated nociceptive neuron sensitization drives OVA-induced VHS. a, Afferent nerve recordings in naive, OVA/infected + saline and OVA/infected + OVA mice ($n = 5$, 6 and 8, respectively). **b**, Rheobase (top) and action potential (AP) number at 2× rheobase (bottom) in DRG neurons incubated with supernatants (SN) from OVA/sham + OVA, saline/infected + OVA and OVA/infected + OVA mice ($n = 20$ neurons (5 supernatants), 18 (6) and 19 (5), respectively). **c**, Ratiometric Ca^{2+} response (left) and percentage of cells that responded to 10 nM capsaicin ('responders', right) in DRG neurons incubated with RPMI medium, histamine, or supernatants from OVA/infected + saline and OVA/infected + OVA mice ($n = 85$ neurons (5 media), 59 (6 solutions), 123 (12 supernatants) and 82 (11 supernatants), respectively). **d**, **e**, Rheobase (left) and action potential number at 2× rheobase (right) (**d**; $n = 19$ neurons (4 supernatants) and 20 (5), respectively) and ratiometric Ca^{2+} response (left) and percentage of cells that responded to 10 nM capsaicin (right) (**e**; $n = 65$ neurons (12 supernatants), 87 (11), 51 (3) and 100 (8), respectively) in DRG neurons incubated with supernatants from VHS mice with vehicle or pyrilamine and (in **e**) comparing wild-type and *Hrh1*$^{-/-}$ neurons. **f**, **g**, VMR to colorectal distention (measured as area under the curve (AUC); % × ml) in OVA/infected + OVA mice treated with vehicle or pyrilamine (**f**, $n = 9$ and 8, respectively) and with wild-type or *Hrh1*$^{-/-}$ background (**g**, $n = 13$ and 9, respectively). *P* values shown in plots. **a**, **b**, One-way ANOVA with Sidak's multiple comparisons test; **c** (left), Kruskal–Wallis test with Dunn's multiple-comparison test; **c** (right), **e** (right), two-tailed Fisher's exact test; **d**, two-tailed *t*-test; **e** (left), two-tailed Mann–Whitney test; **f**, **g**, two-way repeated measures ANOVA with Sidak's multiple comparisons test. **a**, **f**, **g**, Median ± IQR; **b** (top), **c** (left), **d** (left), **e** (left), box plots (centre line, median; box, 25th–75th percentiles; whiskers, 10th–90th percentiles); **b** (bottom), **d** (right), violin plots (centre line, median).

(Extended Data Fig. 6i) and SEB-VHS mice did not develop ear swelling after intradermal injection of OVA (Extended Data Fig. 6j), indicating a local but not a systemic immune response to OVA. To evaluate whether SAgs were also involved in the pathogenesis of IBS, we compared the presence of the main SAg-producing bacteria (*Staphylococcus aureus* and *Streptococcus pyogenes*[18]) in faecal samples from patients and healthy volunteers. Notably, 23% of the faecal samples from patients with IBS tested positive for *S. aureus*, compared to 9% of samples from healthy volunteers (Extended Data Fig. 6k). Moreover, 47% of the positive IBS samples were positive for one or more SAgs compared to 17% of those from healthy volunteers. Previous studies have linked *S. aureus* colonization to conditions associated with antigen-specific sensitization, such as allergic rhinitis, asthma and food allergy[19]. Thus, we speculate that SAgs might be involved in initiating VHS in subsets of patients with IBS.

After characterizing the mechanisms underlying food-mediated VHS in two pre-clinical models, we investigated whether a similar process is present in individuals with IBS. To evaluate whether food antigens can indeed evoke a localized immune response in the colon, we injected solutions of soy, wheat, gluten and milk into the rectosigmoid mucosa of 12 individuals with IBS and 8 healthy volunteers (Supplementary Video 1). None of the participants was allergic to these dietary antigens (Extended Data Table 2). Notably, all 12 of the IBS group showed mucosal reactions to at least one of the food antigens tested (Fig. 4a, b, Supplementary Videos 2–4), whereas only two healthy volunteers showed single positive reactions (one to soy and one to gluten). Next, we assessed tryptase activity as a proxy for mast cell degranulation. Under basal conditions, total trypsin-like-activity was higher in individuals with IBS than in healthy volunteers (Extended Data Fig. 7a), as previously described[20], and tryptase activity, discriminated from overall activity by using the specific inhibitor APC-366, was higher after injection of histamine, soy, wheat and gluten (Fig. 4c). AEBSF (a broad-spectrum serine protease inhibitor) completely inhibited trypsin-like activity. Finally, while we found no differences in the total number of mast cells or IgE^+ mast cells (Extended Data Fig. 7b, c), individuals with IBS had more IgE^+ mast cells close to nerve fibres (≤5 µm) (Extended Data Fig. 7d), in keeping with previous findings[21]. The distance between IgE^+ mast cells and nerve fibres was smaller in individuals with IBS than in healthy volunteers (Fig. 4d, e), and was inversely correlated with the severity of abdominal pain (Fig. 4f). Mast cell IgE immunofluorescence intensity was higher in individuals with IBS than in healthy volunteers (Fig. 4g, h) and positively correlated with both severity of abdominal pain (Fig. 4i) and the diameter of mucosal oedema (Extended Data Fig. 7e). Deep sequencing of immunoglobulin genes using tissue cDNA from biopsies showed that individuals with IBS and healthy volunteers had similar numbers of IgE^+ clones (Extended Data Fig. 7f). Evaluation of allergen-specific clonal populations will be needed to further explore potential local sources of pathogenic IgE. Together, these results suggest that, similar to our pre-clinical models, food antigens trigger mast cell activation in patients with IBS, probably through a local IgE-mediated mechanism.

A key breakthrough proposed here is the understanding of how oral tolerance to food antigens, a pivotal regulatory process in

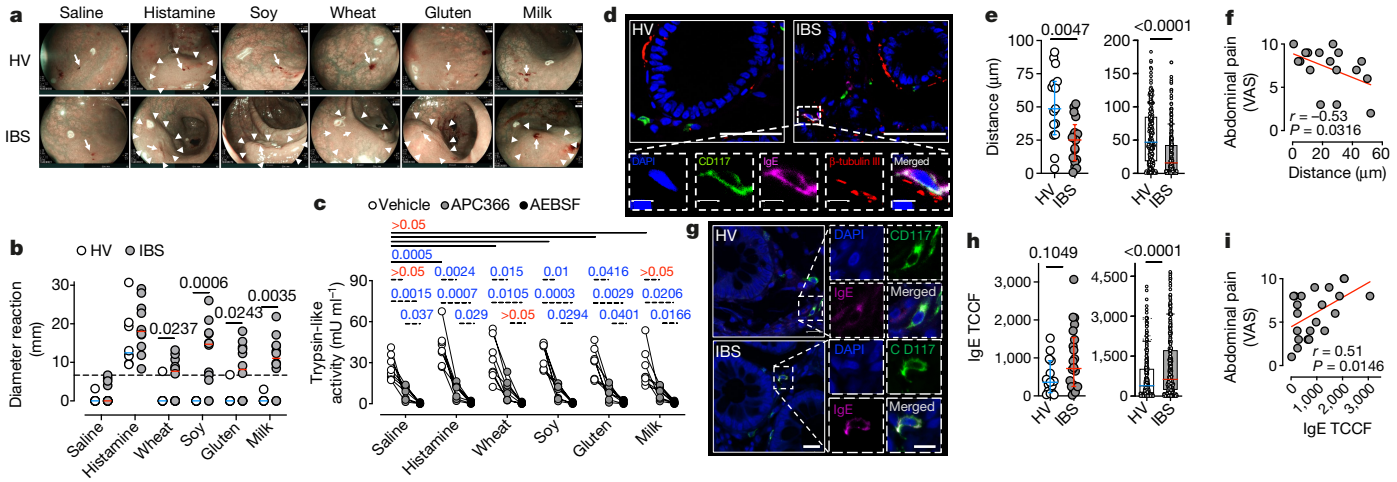

Fig. 4 | Intramucosal injection of food antigens induces an immediate mucosal response in patients with IBS. a, **b**, Representative images (**a**; arrows, antigen injection sites; arrowheads, reaction areas) and diameters of reactions to food antigens injected into healthy volunteers (HV) and individuals with IBS ($n = 8$ and 12, respectively; dotted line in **b** represents the threshold for positive reactions). **c**, Trypsin-like activity in supernatants from rectal biopsies taken after antigen injection in individuals with IBS ($n = 8$). **d**, **e**, Examples of micrographs (**d**) used to measure distance from IgE$^+$ mast cells to nerve fibres (**e**) in healthy volunteers ($n = 15$ individuals (left), 206 cells (right)) and individuals with IBS ($n = 17$ individuals (left), 296 cells (right)). Scale bars, 50 μm (top), 5 μm (bottom). **f**, Correlation between distance from IgE$^+$ mast cells to nerve fibres and abdominal pain severity in individuals with IBS ($n = 17$). VAS, visual analogue scale. **g**, **h**, Examples of micrographs (**g**) used to quantify IgE intensity (TCCF) in mast cells (**h**) in mucosal rectal biopsies from healthy volunteers ($n = 15$ individuals (left), 261 cells (right)) and individuals with IBS ($n = 22$ individuals (left), 315 cells (right)). Scale bars, 20 μm (left), 10 μm (right). **i**, Correlation between the IgE TCCF and abdominal pain severity in individuals with IBS ($n = 22$). *P* values shown in plots. **b**, **e**, **h**, Two-tailed Mann–Whitney test; **c**, two-way ANOVA with Sidak's multiple-comparisons test; **f**, two-tailed Spearman's correlation; **i**, two-tailed Pearson's correlation. **b**, Individual data points and median; **e** (left), **h** (left), median ± IQR; **e** (right), **h** (right), box plots (centre line, median; box, 25th–75th percentiles; whiskers, 10th–90th percentiles).

homeostasis, can be lost in IBS and lead to aberrant pain signalling. We provide evidence that local IgE antibodies are involved in food-induced abdominal pain (Extended Data Fig. 8). A fundamental difference from food allergy is that OVA-specific IgE antibodies were detectable only in colonic tissue, indicating a local rather than systemic immune response against dietary antigens. A role for local IgE antibodies has previously been demonstrated in the airways, in particular in patients with allergic rhinitis and chronic rhinosinusitis with nasal polyps[22], and they are associated with increased airway reactivity. Based on our data, we propose that IBS, at least in an immunogenetically susceptible subgroup of patients, is part of a spectrum of food-induced disorders mediated by mast cell activation, with systemic food allergy at the extreme end of the spectrum. The risk of developing IBS is likely to depend on genetic make-up, favouring an atopic immune response. This hypothesis is further supported by the association of IBS with atopic diseases such as allergic rhinitis, allergic eczema and asthma[23,24]. Whether this concept also explains IBS-like symptoms reported by patients with inflammatory bowel disease in clinical remission[25] remains unclear, but is certainly of great interest.

The concept of food-mediated VHS proposed herein has important implications with respect to the development of treatments for IBS and related disorders. Blocking the effects of mast cell mediators, as with the H_1R-antagonist ebastine[14], may be effective, particularly when using compounds that target upstream mechanisms that lead to mast cell sensitization and activation. Thus, IgE-mediated activation of mast cells could be of interest as a prognostic biomarker as well as a therapeutic target in patients with IBS. Along the same lines, improvement of IBS symptoms has been described in patients with severe asthma treated with omalizumab, a monoclonal antibody against IgE[26]. Therefore, our findings set the stage for further studies of the potential of therapies that target upstream mechanisms of mast cell sensitization and/or activation, such as IgE neutralization or inhibitors of spleen tyrosine kinase—a pivotal signalling transducer that couples antigen–IgE/FcεRI complexes, which regulate mast cell degranulation[27].

Online content

Any methods, additional references, Nature Research reporting summaries, source data, extended data, supplementary information, acknowledgements, peer review information; details of author contributions and competing interests; and statements of data and code availability are available at https://doi.org/10.1038/s41586-020-03118-2.

1. Schäfer, T. et al. Epidemiology of food allergy/food intolerance in adults: associations with other manifestations of atopy. *Allergy* **56**, 1172–1179 (2001).
2. Honda, K. & Littman, D. R. The microbiota in adaptive immune homeostasis and disease. *Nature* **535**, 75–84 (2016).
3. Mowat, A. M. I. Anatomical basis of tolerance and immunity to intestinal antigens. *Nat. Rev. Immunol.* **3**, 331–341 (2003).
4. Bouziat, R. et al. Reovirus infection triggers inflammatory responses to dietary antigens and development of celiac disease. *Science* **356**, 44–50 (2017).
5. Spiller, R. & Garsed, K. Postinfectious irritable bowel syndrome. *Gastroenterology* **136**, 1979–1988 (2009).
6. Card, T. et al. Post-infectious IBS: defining its clinical features and prognosis using an internet-based survey. *United European Gastroenterol. J.* **6**, 1245–1253 (2018).
7. Ford, A. C., Lacy, B. E. & Talley, N. J. Irritable bowel syndrome. *N. Engl. J. Med.* **376**, 2566–2578 (2017).
8. Barbara, G. et al. Mast cell-dependent excitation of visceral-nociceptive sensory neurons in irritable bowel syndrome. *Gastroenterology* **132**, 26–37 (2007).
9. Seiffart, V. et al. IL10-deficiency in CD4$^+$ T cells exacerbates the IFNγ and IL17 response during bacteria induced colitis. *Cell. Physiol. Biochem.* **36**, 1259–1273 (2015).
10. Mondelaers, S. U. et al. Effect of genetic background and postinfectious stress on visceral sensitivity in *Citrobacter rodentium*-infected mice. *Neurogastroenterol. Motil.* **28**, 647–658 (2016).
11. Lee, J. W. et al. Subjects with diarrhea-predominant IBS have increased rectal permeability responsive to tryptase. *Dig. Dis. Sci.* **55**, 2922–2928 (2010).
12. Wu, Y. L., Stubbington, M. J. T., Daly, M., Teichmann, S. A. & Rada, C. Intrinsic transcriptional heterogeneity in B cells controls early class switching to IgE. *J. Exp. Med.* **214**, 183–196 (2017).
13. Kassinen, A. et al. The fecal microbiota of irritable bowel syndrome patients differs significantly from that of healthy subjects. *Gastroenterology* **133**, 24–33 (2007).
14. Wouters, M. M. et al. Histamine receptor H1-mediated sensitization of TRPV1 mediates visceral hypersensitivity and symptoms in patients with irritable bowel syndrome. *Gastroenterology* **150**, 875–887.e9 (2016).

15. Hughes, P. A. et al. Post-inflammatory colonic afferent sensitisation: different subtypes, different pathways and different time courses. *Gut* **58**, 1333–1341 (2009).
16. Liu, J. N. et al. The prevalence of serum specific IgE to superantigens in asthma and allergic rhinitis patients. *Allergy Asthma Immunol. Res.* **6**, 263–266 (2014).
17. Forbes-Blom, E., Camberis, M., Prout, M., Tang, S. C. & Le Gros, G. Staphylococcal-derived superantigen enhances peanut induced Th2 responses in the skin. *Clin. Exp. Allergy* **42**, 305–314 (2012).
18. Proft, T. & Fraser, J. D. Bacterial superantigens. *Clin. Exp. Immunol.* **133**, 299–306 (2003).
19. Jones, A. L., Curran-Everett, D. & Leung, D. Y. M. Food allergy is associated with *Staphylococcus aureus* colonization in children with atopic dermatitis. *J. Allergy Clin. Immunol.* **137**, 1247–1248.e3 (2016).
20. Rolland-Fourcade, C. et al. Epithelial expression and function of trypsin-3 in irritable bowel syndrome. *Gut* **66**, 1767–1778 (2017).
21. Barbara, G. et al. Activated mast cells in proximity to colonic nerves correlate with abdominal pain in irritable bowel syndrome. *Gastroenterology* **126**, 693–702 (2004).
22. De Schryver, E. et al. Local immunoglobulin e in the nasal mucosa: clinical implications. *Allergy Asthma Immunol. Res.* **7**, 321–331 (2015).
23. Tobin, M. C. et al. Atopic irritable bowel syndrome: a novel subgroup of irritable bowel syndrome with allergic manifestations. *Ann. Allergy Asthma Immunol.* **100**, 49–53 (2008).
24. Jones, M. P., Walker, M. M., Ford, A. C. & Talley, N. J. The overlap of atopy and functional gastrointestinal disorders among 23,471 patients in primary care. *Aliment. Pharmacol. Ther.* **40**, 382–391 (2014).
25. Halpin, S. J. & Ford, A. C. Prevalence of symptoms meeting criteria for irritable bowel syndrome in inflammatory bowel disease: systematic review and meta-analysis. *Am. J. Gastroenterol.* **107**, 1474–1482 (2012).
26. Pearson, J. S., Niven, R. M., Meng, J., Atarodi, S. & Whorwell, P. J. Immunoglobulin E in irritable bowel syndrome: another target for treatment? A case report and literature review. *Therap. Adv. Gastroenterol.* **8**, 270–277 (2015).
27. Gilfillan, A. M. & Rivera, J. The tyrosine kinase network regulating mast cell activation. *Immunol. Rev.* **228**, 149–169 (2009).

Methods

Study participants

All experiments involving humans and human material were approved by the Medical Ethics Committee of the University Hospitals Leuven and all human participants provided informed consent (reference approval numbers: S51973, S55484 and S55485).

Food antigen injections. Eight healthy volunteers (female, median 50 years of age (IQR 32–54)) who were free of abdominal symptoms, with no history of gastrointestinal disease or previous gastrointestinal surgery and not taking gastrointestinal medication, were recruited by public advertisement. Twelve participants with IBS meeting the ROME III criteria[28] (eight females, median 29 years of age (IQR 21–39)) were recruited from the outpatient clinic of the University Hospitals Leuven. Allergy to soy, wheat, gluten and milk was excluded in all participants (by anamnesis, skin-prick test and total IgE, tryptase and antigen-specific IgE in serum performed by a trained allergologist).

Trypsin-like activity. Thirteen healthy volunteers (ten females, median 29 years of age (IQR 23–47)) were recruited by public advertisement. They were free of abdominal symptoms, had no gastrointestinal disease or surgery and were not on gastrointestinal medication. Forty-eight individuals with IBS meeting the ROME III criteria (33 females, median 31 years of age (IQR 19–40)) were recruited from the outpatient clinic of the University Hospitals Leuven.

Bacterial identification in faecal samples. Sixty-four healthy volunteers (35 females, median 49 years of age (IQR 32–58)) were recruited by public advertisement. They were free of abdominal symptoms, had no gastrointestinal disease or surgery and were not on gastrointestinal medication. Eighty-four individuals with IBS meeting the ROME III criteria (66 females, median 38 years of age (IQR 25–50)) were recruited from the outpatient clinic of the University Hospitals Leuven.

Biopsy collection for immunofluorescence staining. Fifteen healthy volunteers (13 females, median 41 years of age (IQR 32–52)) were recruited by public advertisement. They were free of abdominal symptoms, had no gastrointestinal disease or surgery and were not on gastrointestinal medication. Twenty-two individuals with IBS meeting the ROME III criteria (20 females, median 31 years of age (IQR 27–43)) were recruited from the outpatient clinic of the University Hospitals Leuven. All participants were invited to report their gastrointestinal symptoms by means of an adapted version of the visual analogue scale (VAS) for IBS[29], assessing the intensity of their last episode of abdominal pain, abdominal discomfort and bloating (scored from 0 to 10).

Mice

All animal experiments were performed in accordance with the European Community Council or Canadian Council of Animal Care guidelines and approved by the Animal Care and Animal Experiments Committee of the Medical Faculty of the KU Leuven or Queen's University Animal Care Committee. Six- to seven-week-old wild-type male BALB/c mice were purchased from Janvier. Six- to seven-week-old male *Cpa3*$^{Cre/+}$ and wild-type male littermates on the BALB/c background[30] were used to study the role of mast cells. Six- to ten-week-old female *Igh7*$^{-/-}$ mice (lacking IgE)[31] on the BALB/c background were used to study the role of IgE, and were compared to wild-type female BALB/c mice. Six- to ten-week-old male *Hrh1*$^{-/-}$ knockout mice on the BALB/c background (Oriental Bioservice, Kyoto, Japan) were used to study the role of the histamine 1 receptor. Mice were maintained under a 14 h–10 h dark–light cycle at a temperature of 20–22 °C (45–70% humidity), and were provided with food and water ad libitum.

Intramucosal injection of food antigens

Individuals with IBS and healthy volunteers were invited to undergo a sigmoidoscopy. During the procedure, food antigens were dissolved in 0.9% NaCl and 200 µl was injected into the rectal mucosa (soy, 3 mg ml^{-1}; wheat, 3 mg ml^{-1}; gluten, 3 mg ml^{-1}; milk, 30 mg ml^{-1}). NaCl (0.9%) and histamine (30 µg ml^{-1}) were used as negative and positive controls, respectively. Sigmoidoscopy was video-recorded and images of the injection sites were taken before injection, immediately after injection, and 12 min after injection. The diameter of mucosal oedema was measured upon blinded evaluation of images taken 12 min after injection, performed independently by two researchers (J.A.-L. and D.B.). The 95th percentile of the reaction diameters for the negative control (saline) was used as the threshold for determining a positive reaction. Moreover, biopsies of the injection site were collected. Next, to obtain biopsy supernatant for protease activity assays, biopsies from eight individuals with IBS injected with different food antigens or controls were incubated in Ad-DMEM/F12 supplemented with GlutaMAX (2 mM), penicillin, streptomycin, gentamycin and amphotericin B (100 U, 100 µg, 10 µg and 0.25 µg per ml, respectively; Invitrogen) for 1 h at 37 °C with 5% CO_2.

C. rodentium infection

C. rodentium (DBS100, ATCC 51459) was cultured overnight in Luria-Bertani (LB) broth medium (MP Biomedicals) at 37 °C, orbital shaking at 180–200 rpm. After 16 h, the bacteria were centrifuged (4 °C, 2,000 rpm, 10 min), the supernatant was discarded, and the pellet was resuspended in fresh LB medium. Eight- to nine-week-old mice were infected by oral gavage with 1×10^9 colony forming units (CFU) of *C. rodentium* or sterile 0.9% NaCl (B. Braun Medical NV/SA).

Telemetric VMR recordings

Six- to seven-week-old mice weighing at least 20 g were implanted with Physiotel ETA-F10 telemetric transmitters (Data Sciences International). In anaesthetized mice (20 mg kg^{-1} ketamine (Nimatek, Eyurovet Animal Health B.V.) and 1 mg kg^{-1} xylazine (Rompun 2%, Bayer)), transmitters were inserted into the abdominal cavity and electrodes were tunnelled through the abdominal wall and sutured into the left external abdominal oblique muscle[10].

As previously described[10], colorectal distensions were performed to evoke abdominal cramping as a read-out of visceral pain, using a distension catheter (volumes from 20 to 80 µl, Fogarty catheter for arterial embolectomy, 4F; Edwards Lifesciences; Extended Data Fig. 1h). Data were calculated as percentage VMR relative to maximum distention response before infection (that is, 80 µl distension was set at 100%) or as area under the curve (AUC) of the four distention volumes. Acknowledge 3.2.6 software was used for analysis.

Compliance

Colonic compliance was studied in order to exclude inflammation-mediated or pharmacologically mediated changes in wall stiffness that could influence nociception in the mice. Thus, the volume–pressure relationship of the colon was evaluated in animals subjected to VMR recordings (Extended Data Table 1).

Post-infection protocol

Two weeks after telemetric transmitter implantation (at 8–9 weeks old), mice were infected with *C. rodentium* as above. Three hours after infection, mice were orally gavaged with 50 mg OVA (grade II, Sigma-Aldrich) dissolved in 0.9% NaCl. Next, OVA was dissolved in drinking water (1% v/v) and changed daily for 10 days after infection. Five weeks after infection, mice were re-exposed to OVA (50 mg) by oral gavage every other day until they were killed. VMRs were recorded before the infection (baseline), 2 and 4 weeks after infection, and 1 h after the 4th and 8th OVA gavages (Fig. 1a). Oral OVA gavage continued every other day until

the day of death (normally after an extra one or two oral OVA challenges, unless otherwise specified; that is, VMR in long-term VHS following final OVA re-exposure, ex vivo re-exposure, and so on). Development of VHS at 7 weeks after infection was routinely confirmed in OVA/infected + OVA mice throughout all experiments. Mice were killed by CO_2 intoxication. In the experiment to evaluate the antigen-specificity of the immune response to OVA, mice received repeated gavages with 50 mg BSA (Enzo Life sciences) dissolved in 0.9% NaCl. In the experiment using *Cpa3*$^{Cre/+}$ mice, OVA re-exposure started 7 weeks after infection, after normalization of infection-induced VHS (which was confirmed at 6 weeks after infection).

Post-infection protocol with previous OVA tolerization

Two weeks before the infection with *C. rodentium*, mice were exposed to 1 mg ml^{-1} OVA in drinking water (low dose oral tolerance) for seven days or were orally gavaged three times, every other day, with 50 mg of OVA (high dose oral tolerance). Following tolerization, mice underwent the same post-infection protocol as described above.

Staphylococcal enterotoxin B protocol

Mice were exposed by oral gavage to 10 µg SEB from *S. aureus* (Sigma-Aldrich) in the presence of 50 mg OVA on three consecutive days. Similar to the post-infection protocol, five weeks after administration of OVA and SEB, mice were re-exposed to OVA (50 mg). VMRs were measured at different time-points: before SEB administration (baseline) and after OVA re-exposure (Extended Data Fig. 5a). Mice were killed by CO_2 intoxication.

Ovalbumin allergy protocol

Six- to eight-week-old BALB/c mice were sensitized on days 0 and 14 with 100 µg OVA (grade V) in the presence of 1 mg Alum (ThermoFisher Scientific Inc.) by intraperitoneal (i.p.) injection. From day 28, mice were challenged every other day with OVA (grade II, 50 mg) by oral gavage.

Mouse treatments

Antibiotics. To overcome the problem of mice refraining from drinking owing to the taste of some antibiotics, we used an adapted protocol[32]. All antibiotics were simultaneously administered by gavage. Ampicillin (25 mg ml^{-1}, Sigma-Aldrich), vancomycin (12.5 mg ml^{-1}, Sigma-Aldrich), neomycin (25 mg ml^{-1}, Sigma-Aldrich) and metronidazole (25 mg ml^{-1}, Sigma-Aldrich) were dissolved in 0.9% NaCl and a volume of 10 ml kg^{-1} body weight was orally gavaged every day from week 4 after the infection with *C. rodentium* until death (Extended Data Fig. 2e). The antibiotic cocktail was prepared fresh every day. When administered with OVA (250 mg ml^{-1}) during the re-exposure, OVA was dissolved and gavaged together with the antibiotic cocktail. NaCl (0.9%) was used as vehicle treatment. The absence of cultivable bacteria in antibiotic-treated mice was confirmed by culturing of faecal pellets in LB agar incubated for 24 h at 37 °C.

Mast cell stabilizer. Doxantrazole (Sigma-Aldrich) was dissolved in $NaHCO_3$ (0.5% w/v) by sonication for 25 min. Mice were treated i.p. with doxantrazole (16.5 mg kg^{-1}) daily 1 h before the OVA re-exposure on 7 consecutive days. $NaCHO_3$ (0.5% w/v) was used as vehicle treatment.

B cell depletion. The B cell-depleting antibody IgG2a anti-CD20 (clone 5D2, isotype IgG2a) and the control antibody (clone 3E5, isotype IgG2a) were kindly provided by Genentech. Mice were treated i.p. with anti-CD20 or control antibody (8 mg kg^{-1}) dissolved in PBS every other day[33] from 4 weeks after the infection with *C. rodentium* until death (Extended Data Fig. 4h).

Plasma cell depletion. Bortezomib (Selleckchem) was dissolved in PBS (DMSO 0.1% v/v). Mice were treated i.p. with bortezomib (0.65 mg kg^{-1})[34] every day from 4 weeks after the infection with *C. rodentium* until death. PBS (DMSO 0.1% v/v) was used as vehicle treatment (Extended Data Fig. 4h).

Anti-IgE antibody. Anti-IgE antibody (clone R1E4, Kerafast) was dissolved in NaCl (0.9%). Mice were treated i.p. with anti-IgE antibody (1 mg kg^{-1}) once a week starting before the re-exposure until death. NaCl (0.9%) was used as vehicle treatment.

Pyrilamine. Pyrilamine maleate salt (Sigma-Aldrich) was dissolved in 0.9% NaCl. Mice were treated i.p. with pyrilamine (5 mg kg^{-1})[35] every other day 1 h before OVA re-exposure until the end of the experiment. NaCl (0.9%) was used as vehicle treatment.

Monoclonal OVA-specific IgE antibody. Mouse anti-OVA monoclonal IgE antibody (clone E-C1, Chondrex) was diluted in PBS. Mice were treated i.p. with OVA-specific IgE antibody (10 µg per mouse) two and one days before the first OVA exposure, and one day before the fourth OVA exposure (Extended Data Fig. 1n). After OVA-specific IgE antibody injection, mice were orally gavaged with OVA four times. A monoclonal anti-dinitrophenyl (DNP) antibody (clone SPE-7, Sigma) was used as a non-specific IgE control antibody.

Diarrhoea development

Diarrhoea score. Mice were placed in a metabolic cage provided with water for 1 h after OVA gavage. Diarrhoea was scored as follows: 1 = normal and dry pellet; 2 = normal and wetter pellet; 3 = wet and less-shaped pellet; 4 = complete diarrhoea.

Whole-gut transit time. Carmine red dye (6%) was dissolved in methylcellulose (0.5% w/v) and orally gavaged to overnight (12-h) fasted mice. Then, mice were individually placed in cages and time was monitored until the appearance of the first faecal pellet containing carmine red dye.

Water content assessment. Faecal pellets were collected after the whole-gut transit time experiment (2 h after carmine dye gavage) and weighed. Next, samples were again weighed after 24-h-incubation at 50 °C (with the Eppendorf tube lid open), and water content was determined (calculated as weight %).

ELISA OVA-specific IgE

Micro-titre plates were coated with 40 µg ml^{-1} OVA (grade V) in carbonate buffer and incubated at 4 °C overnight. Next, plates were blocked for 2 h at room temperature with PBS containing 3% BSA. Next, plates were loaded with 50 µl sample and incubated overnight at 4 °C. Then, plates were incubated for 1 h at room temperature with detection antibody (biotin rat anti-mouse IgE, 4 µg ml^{-1}, BD Biosciences), followed by incubation at room temperature for 30 min with Strep-AP (R&D systems, bipp) (diluted 1:500 in 1% BSA, 0.05% Tween 20, 0.025 M Tris, 0.5M NaCl; pH 7.4). Finally, BluePhos substrate (KPL) was added to the reaction and incubated for 30 min at room temperature. The reaction was stopped with H_2SO_4 (2 M) and the absorbance was measured at a wavelength of 620 nm (A_{620}). Absorbance values were normalized by the amount of protein (mg) measured using a BCA Protein Assay Kit (ThermoFisher Scientific) according to the manufacturer's instructions.

Ear prick allergy test

Mice were subjected to intradermal injections of 1 µg OVA (Grade III, Sigma-Aldrich) dissolved in sterile saline in one ear and 10 µl saline in the other. Ear swelling was compared with a caliper 30 min after injection.

Colonic permeability

Freshly isolated colonic tissue was mounted in Ussing chambers (Mussler Scientific Instruments) with an opening of 0.017 cm^2 and without removal of the seromuscular layer as previously described[36].

Transepithelial electrical resistance was continuously measured (open circuit conditions, bipolar constant-current pulses of 16 μA for 200 ms) and passage of fluorescein sodium salt was assessed every 30 min over 2 h. The concentration of fluorescein was measured using a FLUOstar Omega fluorescence reader (BMG Labtech) and the transepithelial electrical resistance with Clamp software (v9.00) (Mussler Scientific Instruments).

DNA extraction and 16S rRNA gene sequencing

Mouse faecal samples were collected at three time points from the same cohort of mice: before *C. rodentium* infection (baseline), 10 days after infection and after OVA re-exposure. DNA was extracted from ~150 mg of faecal samples using MagAttract PowerMicrobiome DNA/RNA KF kit. The V4 region of 16S rRNA genes was amplified using the 515F/806R primer pair and purified using the QIAquick PCR Purification Kit. Sequencing was performed using the Illumina MiSeq platform (MiSeq Reagent Kit v2).

Microbiome analysis

After demultiplexing with the LotuS 1.565[37], fastq sequences were further processed following the DADA2 microbiome pipeline[38]. In brief, sequence reads were first filtered and trimmed with the parameters: truncQ = 11, truncLen = c (150,200), and trimLeft = c (30, 30). Filtered reads were denoised using the DADA2 algorithm, which infers sequencing errors. After removing chimaeras, an amplicon sequence variants (ASVs) table was constructed and taxonomy was assigned using the Ribosomal Database Project (RDP) classifier implemented in DADA2. Before downstream analysis, bacterial abundances were transformed using centred log-ratio (CLR) transformation of Aitchinson to control the compositionality of the sequencing data (CoDaSeq R package function codaSeq.clr[39]). Zero counts in the AVS table were replaced by multiplicative zero imputation using the zCompositions package function cmultRepl[40]. Ordination analysis (principal component analysis, PCA) with contributing bacteria was performed at genus-level using the vegan R package (functions: *prcomp* and *envfit*; R version 3.4.1)[41]. Association of hypersensitivity with genus *Robinsoniella* and *Eisenbergiella* was assessed using the Mann–Whitney *U*-test. All analyses were performed in R (version 3.4.1).

Histopathology assessment of mouse samples

Samples were fixed in 4% paraformaldehyde (PFA) at 4 °C overnight, transferred to sucrose (0.3 g ml^{-1}) and stored at 4 °C. Samples were embedded using conventional techniques. Five-micrometre sections were cut and stained with haematoxylin and eosin (H&E). Slides were reviewed using an Olympus BX41 light microscope and scored blinded. Crypt length, crypt space and muscle thickness were measured.

Mast cell live imaging in mouse colonic submucosa

The colon was dissected and placed into Krebs solution oxygenated with 95% O_2, 5% CO_2. The colon was cut open parallel to the mesenteric line, cleaned of faecal pellets and pinned flat in a Sylgard plate. Upon removal of the mucosa, the submucosal layer was dissected, placed on a metal ring to stabilize the tissue and loaded with the dye sulforhodamine 101-coupled avidin (8 μg ml^{-1} in Krebs solution, Sigma-Aldrich) for 20 min and washed for 5 min with Krebs solution[42,43]. For image acquisition, the field of interest was selected randomly based on Avidin staining and incubated with OVA peptide 323–339 (10 μg ml^{-1}; InvivoGen). Five *Z*-stacks per section (5 μm depth) were acquired just upon incubation with OVA (0 min) and every 7 min thereafter, for 28 min for Texas red channels using a 25× water immersion lens under a confocal microscope (Zeiss LSM 780, Belgium). All images were acquired using the same settings using Zen (v14.0.20.201) software. Ionomycin (10 μM, Sigma-Aldrich) was used as positive control for mast cell degranulation. For fluorescence intensity analysis, *Z*-stacks were processed (ImageJ 2.0.0-rc-54/1.52d) as sum projection used to quantify total corrected cell fluorescence (TCCF) as previously described[44] and expressed as a percentage compared to TCCF at the baseline (time = 0 min). For calculation of the percentage of mast cells that were degranulated, we used the 95th percentile of TCCF % loss in mast cells from the OVA/sham + OVA group at time = 28 min as a threshold for mast cells to degranulate. Representative images were acquired using a 25× water immersion lens and processed as sum projections. Images were assigned with red colour and adjusted similarly for brightness and contrast.

Quantification of histamine release

The release of histamine was assessed by incubating 5-mm-thick colonic tissue rings (3 rings per well in a 24-well plate) for 60 min (37 °C, 5% CO_2) in 2 ml Krebs buffer supplemented with histamine catabolism inhibitors (10 μM diminazene aceturate, 1 μM *R*-(−)-deprenyl hydrochloride and 10 μM SKF 91488 dihydrochloride) in the presence of 10 μg ml^{-1} $OVA_{323–339}$. Control samples were incubated with vehicle (supplemented Krebs buffer) or 10 μg ml^{-1} $OVA_{257–264}$. Tissue supernatants were collected, cleared by centrifugation (5 min at 12,000*g* at 4 °C) and stored at −80 °C until use. Histamine concentration was measured by enzyme immunoassay (Immunotech #IM2015), and normalized to protein content (nM histamine per mg protein) upon quantification by the BCA method, both according to the supplier's instructions.

RNA extraction and cDNA preparation

The RNeasy Mini Kit (Qiagen) was used to isolate total RNA according to the manufacturer's instructions (Qiagen). cDNA was then transcribed (Quanta Biosciences) and subjected to RT–qPCR analysis according to the manufacturer's instructions.

Tissue harvest for single-cell suspensions

The colon and small intestine were removed from mesenteric fat tissue, opened longitudinally and subsequently cleaned in cold phosphate-buffered saline (PBS) and Hank's balanced salt solution (HBSS; Gibco) supplemented with fetal calf serum (FCS, 1%, Lonza) and penicillin/streptomycin (Gibco) (100 μg ml^{-1}) (wash medium). Epithelial cells were removed by an 8-min incubation on a magnetic stirrer in warm (37 °C) wash medium supplemented with DTT (1 mM) and EDTA (1 mM). After a washing step, tissue was cut into pieces smaller than 3 mm and digested by a 25- to 30-min incubation on a magnetic stirrer in warm (37 °C) minimum essential medium (MEM)-α containing penicillin/streptomycin (100 μg ml^{-1}), β-mercaptoethanol (50 μM, Sigma-Aldrich), FCS (5%), DNase (5 U ml^{-1}, Roche), collagenase V (0.85 mg ml^{-1}, Sigma-Aldrich), collagenase D (1.25 mg ml^{-1}, Roche), dispase (1 mg ml^{-1}, Gibco). After digestion, cells were filtered through a 70-μm cell strainer and lamina propria cells were purified using a Percoll (VWR) gradient (44 to 67%). Purified cells were washed and re-suspended in PBS supplemented with FCS (1%) and penicillin/streptomycin (100 μg ml^{-1}) and stained for flow cytometry.

Flow cytometry

Single-cell suspensions were labelled for flow cytometry analysis using fluorophore-conjugated anti-mouse antibodies for 30 min at 4 °C. Living cells were identified using a viability dye (Fixable Viability Dye eFluor506, eBioscience). For intracellular staining, cells were fixed for 30 min, washed and then permeabilized for 20 min using a Foxp3/Transcription Factor Staining Buffer Set (eBioscience). Cells were incubated with intracellular antibodies for 1 h at 4 °C. Samples were acquired using BD FACSCanto II (BD Biosciences) or BD FACS Symphony A5 (BD Biosciences), and analysis was carried out using FlowJo software (V.10.0.8, BD).

Gene expression quantification

Gene expression in mouse colonic samples by RT–qPCR. All steps were performed according to the manufacturers' instructions and as previously described[10] using a LightCycler 480 multiwell plate 96

(Roche GmBH). Gene expression was calculated as relative quantification of gene expression using the Pfaffl method[45] and normalized to the control group. The primer pairs used are described in Supplementary Table 1. The mRNA expression of each gene was compared to the expression of *Actb* (reference gene).

qPCR identification of *S. aureus* and SAgs in faecal samples. The presence of *S. aureus* and *S. pyogenes* was evaluated by identifying the presence of the *nuc* and *spy1258* genes, respectively. The presence of the following SAgs of *S. aureus* were evaluated: sea, seb, sec, sed, seg, she, sel*k*, sel*l*, sel*m*, sel*o*, sel*p*, sel*q* and sel*u*. The primer pairs used are described in Supplementary Table 1.

mIL-4 enzyme-linked immunospot assay

IL-4 producing cells were quantified by means of enzyme-linked immunospot (ELISpot) assay, according to the manufacturer's instructions (CTL-Europe). Total cells were isolated from colon-draining lymph nodes (cMLN). Cells were seeded (5×10^5 per well in duplicate) on plates pre-coated with capture antibody for mIL-4 in medium (R10) and incubated at 37 °C with 5% CO_2 for 4 days. Medium contained 1% penicillin/streptomycin, 1% L-glutamine and 10% fetal bovine serum. Additionally, R10 contained 50 μM β-mercaptoethanol and 20 mM HEPES. As a positive control, cells were activated with 50 ng ml^{-1} phorbol myristate acetate (PMA) and 500 ng ml^{-1} ionomycin for 4 h before the first washing step. Cytokine-producing cells were resolved by a 25-min-incubation with the Blue Developer Solution provided. Spot-forming cells were quantified with ImmunoSpot software (v7.0; CTL-Europe, Bonn, Germany).

Preparation of colonic supernatants

Supernatants (colonic tissue 2% w/v, collected 7 weeks after infection) were incubated for 4 or 24 h at 37 °C, 5% CO_2 in RPMI (Lonza) supplemented with fetal calf serum (10%), penicillin, streptomycin, gentamycin and amphotericin B (100 U, 100 μg, 10 μg and 0.25 μg per ml, respectively; Invitrogen). Supernatants were collected and stored at −80 °C until use.

Quantification of inflammatory cytokines

Colonic supernatants were analysed for secretion of cytokines (IL-4, IL-6, KC (mouse IL-8 homologue), IL-10, IL-13, IL-17A, IFN-γ, MCP1, TNF) by flow cytometry using BD Cytometric Bead Array (CBA) (BD Biosciences) according to the manufacturer's instructions. Cytokine concentrations were calculated using FCAP Array Software (v3.0; BD Biosciences).

Afferent nerve recording

The colon from BALB/c mice, with the associated lumbar splanchnic nerves, was dissected out. Tissues were placed in a bath perfused with carbogenated Krebs buffer (7 ml min^{-1}; 32–34 °C) and lumbar splanchnic nerves were isolated as previously described[46]. Lumbar splanchnic nerve fibres were identified on the basis of their anatomic location, their receptive field and response to mechanical stimuli such as brush stroking and von Frey hair stroking[46]. Basal mechanosensitivity was characterized using response of receptive fields to von Frey hair probing (0.16 g applied 3 times for 3 s) applied to the colonic mucosa. For analysis, individual single-unit discharge was discriminated offline using template-matching wavemark software. For the mechanosensitivity to von Frey hair probing, peak action potential discharge (Hz) over a 2-s period within the 3-s period of probing was determined for each probe and a mean response was calculated from each set of 3. Spike2 software (V.607) was used for the analysis.

Patch-clamp recording

DRG neurons (T9–T13) from 8–12-week-old mice were bilaterally excised under a dissection microscope as previously described[47]. Following overnight incubation with colonic supernatants, DRG neuronal activity was then assessed using perforated-patch clamp with amphotericin B (0.24 mg ml^{-1}). The composition of the extracellular solution was as follows (in mM): 140 NaCl, 5 KCl, 1 $MgCl_2$, 2 $CaCl_2$, 10 4-(2-hydroxyethyl)-1-piperazineethanesulfonic acid (HEPES), 10 D-glucose; pH 7.4. For the pipette solution (in mM): 110 K-gluconate, 30 KCl, 10 HEPES, 1 $MgCl_2$, 2 $CaCl_2$; pH 7.25. The liquid junction potential was calculated to be 12 mV and corrected. The recording chamber was continuously perfused with external solution at approximately 1–2 ml min^{-1}. Final pipette resistance was 2–5 MΩ in bath solution. Signals were amplified using Multiclamp 700B, digitized by Digidata 1440A converters, and recorded using pClamp 10.5 software (Molecular Devices). Only neurons with resting membrane potentials more negative than −40 mV were analysed. Only neurons with <30 pF capacitance were used because these neurons have been shown to display properties associated with nociceptors[48,49]. Neuronal excitability was measured by recording the rheobase (minimum amount of current required to elicit an action potential) and numbers of action potentials discharged at twice the rheobase, as previously described[50]. The role of the H_1R receptor was evaluated using pyrilamine (1 μM), applied 1 h before application of colonic supernatant.

Ca^{2+} imaging

DRG neurons (T9–T13) from 8–12-week-old mice were bilaterally excised under a dissection microscope and intracellular Ca^{2+} concentration was measured as previously described[14]. Following overnight incubation with colonic supernatants, neurons were loaded with 2 μM Fura-2AM (Invitrogen) for 20 min at 37 °C. The baseline intracellular Ca^{2+} concentration was monitored for 120 s and neurons were perfused with 10 nM of the TRPV1 channel-agonist capsaicin (Sigma-Aldrich) to evaluate neuron sensitization. Capsaicin (1 μM) was used to identify TRPV1-expressing neurons. Neurons were identified upon perfusion with 45 mM K^+Cl^--supplemented Krebs. We previously performed[14] dose–response curves using 10, 30, and 100 nM capsaicin, in the presence or absence of 10 μM histamine. Neurons responding to 10 nM capsaicin were more sensitized by histamine than neurons responding to 30 and 100 nM capsaicin; therefore, the first concentration was chosen for our experiments. The role of the H_1R receptor was evaluated using pyrilamine (1 μM). Pyrilamine was applied to neurons 1 h before application of colonic supernatant and was present throughout the incubation with colonic supernatants. The percentage of neurons that responded to 10 nM capsaicin among the total amount of neurons recorded was calculated. TILLVision software (TILL Photonics) (v4.5.66 build 10002) was used for the analysis.

Colonic tissue homogenates

Immediately after mice were killed, mouse colonic and small intestine tissues were removed, snap frozen and kept frozen while being mechanically disrupted using a TissueLyser II (Qiagen). Disrupted tissues were suspended (10% w/v) in 0.9% NaCl solution containing Protease Inhibitor Tablets (Compete, Roche Diagnostics). After homogenization by vortex, samples were centrifuged and supernatants were collected and stored at −80 °C until use.

DNA extraction from faecal samples

Faecal samples (200 mg) were incubated in Brain Heart Infusion broth (Sigma-Aldrich) for 24 h with shaking at 37 °C, and DNA was extracted using a commercial kit. Thereafter, bacterial DNA was extracted using a Genomic DNA Extraction from Tissue kit following the manufacturer's instructions (Macherey-Nagel) adapted to the Support Protocol for hard-to-lyse bacteria.

SAgs-positive *S. aureus* strains, used as positive controls, were kindly provided by the National Reference Centre (NRC) for *S. aureus* of Université Libre de Bruxelles (ULB) (Belgium).

Immunofluorescence staining, total corrected cell fluorescence and cell distance analyses in human samples

For immunostaining, biopsies were fixed in 4% PFA, then transferred to sucrose (0.3 g ml^{-1}) and subsequently embedded in OCT compound and stored at −80 °C. Cryosections (5 µm) were incubated with 1% BSA in PBS for 1h at room temperature, followed by overnight incubation with the primary antibody at 4 °C. Primary antibodies were prepared in PBS containing 0.3% Triton-X and used to stain mast cells (1:500 anti-CD117 K963; IBL), IgE (1:250 mouse anti-human MHE-18, BioLegend) and nerve fibres (1:500 chicken anti-beta III tubulin, Abcam). After washing, sections were incubated with fluorescent secondary antibodies for 2 h in the dark at room temperature. Secondary antibodies (Jackson ImmunoResearch) included Cy3 donkey anti-rabbit (1:500), Cy5 donkey anti-mouse (1:500) (for immunofluorescence intensity evaluation), Cy3 donkey anti-chicken (1:300), Cy5 donkey anti-rabbit (1:500), and A488 donkey anti mouse (1:500) (for measuring distance between IgE$^+$ mast cells and nerve fibres). Sections were mounted in SlowFade Gold (Life Technologies Europe B.V.) with DAPI. A negative control, absence of primary antibody, was carried out for every subject to ensure antibody specificity. For image acquisition, the field of interest was selected randomly on the basis of DAPI staining and 5–6 *Z*-stacks per section with a step-size of 1.07 µm were acquired for three channels (DAPI, Cy3 and Cy5) using a 40× oil immersion lens under a confocal microscope (Zeiss LSM 880, Airyscan). All images were acquired using the same settings using Zen Black 2.3 SP1 software. For fluorescence intensity analysis, *Z*-stacks were processed (ImageJ 2.0.0-rc-54/1.52d) as sum projection and used to quantify TCCF as previously described[44]. Cells were identified using c-kit immunoreactivity and only nucleated profiles were included for analysis. For distance measurements, *Z*-stacks were processed (ImageJ 2.0.0-rc-54/1.52d) as sum projection and used to quantify the distance from the periphery of nerve fibres (based on beta tubulin staining) to the mast cell periphery (identified based on CD117 staining) by using the straight line tool. Cells were identified using CD117 and only nucleated profiles were included for analysis. Immunostaining, image acquisition and mean fluorescence intensity analysis were performed in a blinded manner. Representative images were acquired using a 63× or 40× oil immersion lens and processes as described above. Images were assigned with pseudo colours (immunofluorescence analysis: green for Cy3 channel and magenta for Cy5 channels; distance analysis: green for Cy5 channel, magenta for A488 channels, red for Cy3 channel) and adjusted for brightness and contrast.

Trypsin-like activity assay

Trypsin-like activity was measured as previously described with some modifications[51,52]. In brief, colonic tissue supernatant samples were incubated with 0.1 mM Tos-GPR-AMC.HCl as substrate in 50 mM Tris, 10 mM $CaCl_2$, pH 8 (Sigma-Aldrich). Substrate cleavage was calculated over 30 min at 37 °C on a FLUOstar Omega microplate reader (BMG Labtech, GmbH). Sample values were interpolated into a linear regression generated with a standard curve of AMC.HCl (0.05–0.5 nmol; Bachem). Mast cell tryptase activity was characterized by pre-incubating supernatants with the specific inhibitor APC-366 (100 µM; Tocris) for 60 min at 37 °C. As controls, samples were pre-incubated with vehicle (0.2% DMSO) or the broad-spectrum serine protease inhibitor AEBSF (1,000 µM; Roche). Data were expressed as mU ml^{-1} (1 U = conversion of 1 nmol of substrate per min).

Library preparation for high-throughput sequencing of immunoglobulin heavy chain genes

cDNA was synthesized from 1 µg RNA using SuperScript III (Thermo Fisher Scientific) and primed with random hexamers (Promega) according to the manufacturer's protocols. IgH genes were amplified by multiplexed RT–PCR using Biomed2 IGHV primers in the FR1 framework region[53] and isotype-specific primers for IgM, IgD, IgG, IgA and IgE located in the CH1 constant region. Each isotype was amplified separately to prevent the formation of cross-isotype chimeric PCR products, and one-tenth of the total pool of cDNA generated from 1 µg of RNA from each sample was used for each RT–PCR reaction. The primer sequences have been published previously[54]. In brief, primers contained 8-mer barcodes used to identify samples as well as half of the Illumina adaptor sequence needed for cluster generation and sequencing on the MiSeq instrument. PCR was performed with gene-specific primers for 35 cycles, and then an additional 12 cycles with primers to complete the Illumina adapters. For Illumina cluster recognition, four randomized nucleotides were included in the primers immediately after the Illumina adaptor sequence in the constant region primers. The PCR programs were as follows: first PCR: 94 °C for 7 min; 35 cycles of (94 °C 30 s, 58 °C 45 s, 72 °C 120 s); and final extension at 72 °C for 10 min; second PCR: 0.4 µl of first PCR product was used as template for this 30-µl reaction. Conditions: 94 °C for 15 min; 12 cycles of (94 °C 30 s, 60 °C 45 s, 72 °C 90 s); and final extension at 72 °C for 10 min. Amplification was confirmed by electrophoresis on agarose gels. To adjust for differences in amplification efficiencies arising from sample quality and biological factors such as low numbers of IgE transcripts relative to IgM, IgD, IgG and IgA transcripts, PCR reactions were pooled in roughly equal amounts based on the visual inspection of band intensity. The pool of products was then separated again by electrophoresis and purified with QIAquick Gel Extraction Kits (Qiagen). IgH libraries were sequenced on an Illumina MiSeq using 600-cycle sequencing kits.

IgH sequence analysis

Paired-end reads were merged by FLASH and sequences with perfect or single mismatch alignment to full-length V_H and C_H primers were demultiplexed according to the primer-encoded barcodes. Isotypes were called by perfect or single mismatch alignment to known constant region gene sequences, to remove artefactual sequences generated by cross-priming in the CH1 region and sequences with low-certainty sub-isotype calls. Out-of-frame rearrangements, rearrangements containing stop codons, and reads with no isotype call were not analysed further. Reads were aligned using a local installation of IgBLAST to identify features including germline *IGHV*, *IGHD* and *IGHJ* genes, framework and heavy chain complementarity determining regions 1, 2 and 3 (CDR-H1, CDR-H2 and CDR-H3). After quality filtering, library sequencing yielded 11,115,260 productively rearranged sequences, which were subsequently clustered into inferred clonal lineages via single linkage clustering, with the restrictions that the sequences had to be from the same individual, use the same *IGHV* gene and the same *IGHJ* gene (disregarding allele call), have the same CDR-H3 length, and have at least 90% identity in the nucleotides encoding the CDR-H3 region. IgE$^+$ clones were defined as those that contained at least one member expressing IgE.

Quantification and statistical analysis

Sample size and statistical methods. For animal studies, the number of mice was selected using power calculations performed on the basis of previous or present studies carried out in our laboratory and in the field. Normal (Gaussian) distribution was determined for all data sets using the Shapiro–Wilk normality test. Datasets where one (or more) group did not pass the normality test (assuming $\alpha = 0.05$) were analysed using non-parametric tests. Otherwise, parametric tests were used. For assessment of the diarrhoea score, whole total transit time and water content in faecal matter we used between 6 and 10 mice per experimental group. For measurement of VMR we used between 3 and 13 mice per experimental group, genotype or pharmacological treatment. For ELISpot assay, we used 4 mice per experimental group. For recording of afferent nerves, we used between 6 and 8 mice per experimental group. For measurement of colonic permeability, we used between 5 and 12 mice per group, genotype or pharmacological treatment. For analysis of gut microbiota, we used 8 mice per experimental group.

For histology studies we used between 6 and 8 mice per experimental group. For measurement of cytokine levels, we used between 8 and 12 mice per experimental group. For measurement of gene expression in mouse colonic samples we used between 5 and 21 mice per experimental group. For FACS analysis we used between 6 and 10 mice per experimental group. For measurement of OVA-specific immunoglobulins we used between 6 and 10 mice per experimental group for serum samples; and between 4 and 19 mice per experimental group for colonic samples. For evaluation of live mast cell degranulation, we analysed 145–239 mast cells per group, from tissue isolated from 6–9 different mice per group. For evaluation of ear-swelling upon OVA intradermal injection we used between 6 and 10 mice per experimental group. For patch-clamp experiments in DRG neurons we used between 18 and 24 neurons per experimental group or pharmacological treatment. For measurement of Ca^{2+} responses we used between 51 and 126 neurons per group, genotype or pharmacological treatment.

In human studies, no power calculations were performed for the food-antigens injection study and the number of participants was chosen on the basis of a previous similar study performed in patients with eosinophilic esophagitis[55]: 8 healthy volunteers and 12 individuals with IBS were used. For the measurement of trypsin-like-activity, samples from the food antigen injection sites of 8 individuals with IBS were processed, and 13 healthy volunteers were compared with 48 individuals with IBS at basal conditions. For assessment of IgE immunofluorescence in mucosal biopsies, we used 15 healthy volunteers and 22 individuals with IBS. For the bacteria and SAg-producing bacteria, the number of samples was chosen based on power calculations of past studies in the field: 64 healthy volunteers and 84 individuals with IBS were used.

Diarrhoea score and colonic compliance were analysed using two-way repeated measures ANOVA with Sidak's multiple-comparisons post-test, and each *P* value was therefore adjusted to account for multiple comparisons. Whole-gut transient time and faecal water content, visceromotor response, afferent nerve recording, measurement of fluorescein sodium and TEER, FACS analysis, OVA-specific IgE in mouse tissue, association between VHS and bacterial abundance, rheobase and action potential number, measurement of Ca^{2+} responses in DRG neurons and total corrected cell fluorescence (TCCF) of IgE in human biopsies were compared using the two-tailed unpaired *t*-test for parametric analyses, or the Mann–Whitney test for nonparametric analyses (see legends). ELISpot mIL-4 was analysed using paired *t*-test of dependent samples. VMRs were also analysed using a two-way repeated measures ANOVA with Sidak's multiple-comparisons post-test, and each *P* value was therefore adjusted to account for multiple comparisons. Measurement of fluorescein sodium and TEER, thickness of muscularis, length crypts, distance between crypts, cytokine levels, gene expression, ear swelling, rheobase, action potential number and measurement of Ca^{2+} responses in DRG neurons were analysed using one-way ANOVA with Sidak's multiple-comparisons post-test for parametric analyses or Kruskal–Wallis test with Dunn's multiple-comparisons post-test for nonparametric analyses (each *P* value was therefore adjusted to account for multiple comparisons). Trypsin-like activity was analysed by two-way ANOVA with Sidak's multiple-comparisons post-test. Associations between IgE immunofluorescence levels and symptom severity scores were assessed by Pearson's correlation and distance between mast cells and IgE^+ nerve fibres and symptom severity scores by Spearman's correlation. Bacteria and SAgs-producing bacteria proportions and proportion of DRG neurons that responded to 10 nM capsaicin were evaluated by two-sided Fisher's exact test. Data were plotted and statistical analysis were performed with Prism (GraphPad Software version 9.0.0, La Jolla, California).

Replication. For VMR recording (except mice receiving repeated BSA by oral gavage, B and plasma cell depletion, treatment with anti-IgE antibody and IgE-deficient mice and treatment with OVA-specific IgE), experiments were performed two or more times and data from individual mice were pooled from all experiments. Diarrhoea score, whole-gut transit time and water content were measured in different batches of animals. Similar numbers of mice were used per experiment, duplicated for control group/treatment and experimental group. For afferent nerve recording and Ussing chambers, experiments were performed twice and data from individual mice were pooled from all experiments. Similar numbers of mice were used per experiment duplicated for control group/treatment and experimental group. All in vivo and ex vivo experiments were routinely assessed on different days, including every group tested on each day. For fluorescence-activated cell sorting (FACS) analysis, at least two experiments were performed for each tissue. For experiments with cultures of DRG neurons, multiple biological replicates were used for each group. For Ca^{2+} experiments (except for $Hrh1^{-/-}$ DRG neurons), experiments were performed twice and neuron Ca^{2+} responses were pooled. For experiments with live mast cell degranulation and histamine release, experiments were performed twice and data were pooled.

Randomization and blinding. For experiments involving transgenic mice and pharmacological treatments, genetically modified mice and wild-type littermates or drug-treated and vehicle/control-treated mice were placed together in the same cages. For pharmacological treatments, the online tool of GraphPad software (QuickCalcs) was used to randomly assign subjects to groups for treatment or vehicle/control.

For pharmacological treatments and experiments with knockout mice, the experimenter recording VMRs was blinded to the treatment and control/vehicle or the mouse genotype and was unblinded for the analysis. For the afferent nerve recording experiment, the experimenter was blinded to the animal groups and was unblinded for the analysis. For the experiments involving cultures of DRG neuron, the experimenters were blinded for the analysis of the neurons and were unblinded for pooling the data in groups and analysing statistical differences. For experiments involving microbiota analysis the experimenter was blinded for the analysis. For experiments involving live mast cell degranulation, the experimenter was blinded during the performance of the experiment and for the analysis of images.

For human experiments, the experimenters analysing the reactions to food antigens were blinded for the image/video analyses and were unblinded once all the reactions had been analysed.

For histopathology assessment of mouse samples and immunostaining in human samples, 5–10 images per sections were randomly captured and analysed by the experimenter in a blinded manner. The experimenter was unblinded for analysis of statistical differences.

For the analysis of immunoglobulin genes from tissue cDNA (IgE^+ clones), the experimenter analysing the number of clones was unblinded only for analysis of statistical differences.

Reporting summary

Further information on research design is available in the Nature Research Reporting Summary linked to this paper.

Data availability

The data for 16S rRNA gene sequences are available from the European Nucleotide Archive (https://www.ebi.ac.uk/ena/) under accession number PRJEB41204. All other relevant data generated and analysed during the current study are available upon reasonable request to the corresponding author. Source data are provided with this paper.

28. Longstreth, G. F. et al. Functional bowel disorders. *Gastroenterology* **130**, 1480–1491 (2006).
29. Bengtsson, M., Persson, J., Sjölund, K. & Ohlsson, B. Further validation of the visual analogue scale for irritable bowel syndrome after use in clinical practice. *Gastroenterol. Nurs.* **36**, 188–198 (2013).
30. Feyerabend, T. B. et al. Cre-mediated cell ablation contests mast cell contribution in models of antibody- and T cell-mediated autoimmunity. *Immunity* **35**, 832–844 (2011).
31. Oettgen, H. C. et al. Active anaphylaxis in IgE-deficient mice. *Nature* **370**, 367–370 (1994).

32. Reikvam, D. H. et al. Depletion of murine intestinal microbiota: effects on gut mucosa and epithelial gene expression. *PLoS ONE* **6**, e17996 (2011).
33. Moritoki, Y. et al. B-cell depletion with anti-CD20 ameliorates autoimmune cholangitis but exacerbates colitis in transforming growth factor-β receptor II dominant negative mice. *Hepatology* **50**, 1893–1903 (2009).
34. Kim, M. S. & Kim, T. S. IgA+ plasma cells in murine intestinal lamina propria as a positive regulator of Treg differentiation. *J. Leukoc. Biol.* **95**, 461–469 (2014).
35. Huang, Z.-L. et al. Altered sleep-wake characteristics and lack of arousal response to H3 receptor antagonist in histamine H1 receptor knockout mice. *Proc. Natl Acad. Sci. USA* **103**, 4687–4692 (2006).
36. Lauffer, A. et al. Subacute stress and chronic stress interact to decrease intestinal barrier function in rats. *Stress* **19**, 225–234 (2016).
37. Hildebrand, F., Tadeo, R., Voigt, A. Y., Bork, P. & Raes, J. LotuS: an efficient and user-friendly OTU processing pipeline. *Microbiome* **2**, 30 (2014).
38. Callahan, B. J. et al. DADA2: high-resolution sample inference from Illumina amplicon data. *Nat. Methods* **13**, 581–583 (2016).
39. Gloor, G. B., Wu, J. R., Pawlowsky-Glahn, V. & Egozcue, J. J. It's all relative: analyzing microbiome data as compositions. *Ann. Epidemiol.* **26**, 322–329 (2016).
40. Palarea-Albaladejo, J. & Martín-Fernández, J. A. ZCompositions – R package for multivariate imputation of left-censored data under a compositional approach. *Chemom. Intell. Lab. Syst.* **143**, 85–96 (2015).
41. Oksanen, J. *et al*. The vegan package. *Community Ecology Package* https://cran.r-project.org/web/packages/vegan/index.html (2008).
42. Reber, L. L. *et al*. Imaging protective mast cells in living mice during severe contact hypersensitivity. *JCI Insight* **2**, e92900 (2017).
43. Joulia, R. et al. Mast cells form antibody-dependent degranulatory synapse for dedicated secretion and defence. *Nat. Commun.* **6**, 6174 (2015).
44. McCloy, R. A. et al. Partial inhibition of Cdk1 in G 2 phase overrides the SAC and decouples mitotic events. *Cell Cycle* **13**, 1400–1412 (2014).
45. Pfaffl, M. W. A new mathematical model for relative quantification in real-time RT-PCR. *Nucleic Acids Res.* **29**, e45 (2001).
46. Brierley, S. M., Jones, R. C. W., III, Gebhart, G. F. & Blackshaw, L. A. Splanchnic and pelvic mechanosensory afferents signal different qualities of colonic stimuli in mice. *Gastroenterology* **127**, 166–178 (2004).
47. Ibeakanma, C. & Vanner, S. TNFα is a key mediator of the pronociceptive effects of mucosal supernatant from human ulcerative colitis on colonic DRG neurons. *Gut* **59**, 612–621 (2010).
48. Stewart, T., Beyak, M. J. & Vanner, S. Ileitis modulates potassium and sodium currents in guinea pig dorsal root ganglia sensory neurons. *J. Physiol. (Lond.)* **552**, 797–807 (2003).
49. Moore, B. A., Stewart, T. M. R., Hill, C. & Vanner, S. J. TNBS ileitis evokes hyperexcitability and changes in ionic membrane properties of nociceptive DRG neurons. Am. *J. Physiol. Gastrointest. Liver Physiol.* **282**, G1045–G1051 (2002).
50. Ibeakanma, C. et al. Brain-gut interactions increase peripheral nociceptive signaling in mice with postinfectious irritable bowel syndrome. *Gastroenterology* **141**, 2098–2108.e5 (2011).
51. Denadai-Souza, A. et al. Functional proteomic profiling of secreted serine proteases in health and inflammatory bowel disease. *Sci. Rep.* **8**, 7834 (2018).
52. Denadai-Souza, A. et al. Effect of tryptase inhibition on joint inflammation: a pharmacological and lentivirus-mediated gene transfer study. *Arthritis Res. Ther.* **19**, 124 (2017).
53. van Dongen, J. J. et al. Design and standardization of PCR primers and protocols for detection of clonal immunoglobulin and T-cell receptor gene recombinations in suspect lymphoproliferations: report of the BIOMED-2 Concerted Action BMH4-CT98-3936. *Leukemia* **17**, 2257–2317 (2003).
54. Roskin, K. M. et al. IgH sequences in common variable immune deficiency reveal altered B cell development and selection. *Sci. Transl. Med.* **7**, 302ra135 (2015).
55. Warners, M. J. et al. Abnormal responses to local esophageal food allergen injections in adult patients with eosinophilic esophagitis. *Gastroenterology* **154**, 57–60.e2 (2018).

Acknowledgements We thank I. Croux and R. De Keyser for technical assistance; L. Beullens, A. W. Essilfie, H. Willekens and H. Volkaerts for nursing assistance in the studies involving human subjects; M. Rasulova for assistance with ELISpot plate read-out; and the Cell and Tissue Imaging Cluster for the use of the NIKON inverted TillVision microscope, epifluorescence microscope BX 41 Olympus and Zeiss LSM880—Airyscan—and Zeiss LSM 780—SP Mai Tai HP DS—confocal microscopes (Cell and Tissue Imaging Cluster, CIC, supported by Hercules AKUL/15/37_GOH1816N and FWO G.0929.15 to P. Vanden Berghe). Flow cytometry was done at the FACS Core facility (KU Leuven) and we thank P. Andrée Penttila and P. Kumar for technical assistance. We thank the National Reference Centre (NRC) for *S. aureus* of Université Libre de Bruxelles (ULB) for SAgs-positive *S. aureus* strains; and Genentech for the IgG2a anti-CD20 antibody and its isotype control. M.V.F., M.F.V. and D.B. were supported by FWO PhD fellowships (1110019N, 11C2219N and 1127415N, respectively). C. Breynaert is supported by the Clinical Research Fund, University Hospitals, Leuven. J.A.-L., M.M.W., P.J., N.S. and Y.A.A. were supported by FWO postdoctoral fellowships (12X9820N, 1248513N, 12R5219N, 12V3619N and 12H8220N, respectively). During this project J.A.-L. was also previously supported by an FWO PhD fellowship (11Y2116N). T.B.F. and H.-R.R. were supported by SFB-TRR156-A07. S.D.B. is supported by NIH grant NIAID R01 AI125567 and an endowment from the Crown Family Foundation. G.E.B. was funded by a KU Leuven university grant (Global Opportunities for Associations GOA 14.011, C14/18/086) and an FWO grant (G0A9516N).

Author contributions J.A.-L., M.V.F., A.D.-S., M.M.W. and G.E.B. planned and designed the experiments. J.A.-L. and M.V.F. performed mouse infections and pharmacological treatments and carried out in vivo animal protocols. J.A.-L., M.V.F., I.A. and M.C.-E. performed immunoglobulin ELISAs. J.A.-L., M.C.-E. and S.U.M. performed diarrhoea-development experiments. J.A.-L. recorded VMRs and compliance, except for pyrilamine treatment and in *Hrh1*$^{-/-}$ mice, which were performed by M.V.F. E.P. performed afferent nerve recordings. J.A.-L. performed colonic permeability assessments, assisted by R.F. J. Si and J.R. performed analysis of murine microbiota. M.V.F. and S.T. performed histopathology assessments in mouse samples. N.S. performed cytokine quantification by cytometric bead array. J.A.-L., I.A. and N.F. performed RNA extraction and quantitative PCR experiments. M.F.V., M.V.F., I.A., N.F. and G.B. performed FACS experiments, assisted by G.M., S.I.M., C. Bosteels and B.N.L. ELISPOT assay was performed by L.D. and A.D.-S. C.L.-L. and J.J.-P. performed patch-clamp experiments, assisted by D.E.R. J.A.-L. performed Ca^{2+} experiments, assisted by Y.A.A. and K.T. J.A.-L. performed bacterial DNA extraction from faecal samples. P.J. and M.F.V. performed immunofluorescence staining of human samples and total corrected cell fluorescence analysis. P.J. and M.C.-E. performed and analysed immunofluorescence staining of mouse samples and mast cell live imaging analysis. R.B., G.E.B., K.V.B. and D.B. performed food antigen injections and collection of biopsies. J.A.-L. and D.B. performed the analysis of the reactions to food antigens. C. Breynaert and R.S. performed the allergy work-up in humans. A.D.-S. designed, performed and analysed protease activity assays. A.D.-S. and M.N. evaluated histamine presence in mouse and human samples, assisted by D.C. and P.A. IgH sequence analysis of IgE^{+} clones was performed by R.A.H., assisted by S.D.B. T.B.F. and H.-R.R. provided *Cpa3*$^{Cre/+}$ mice, and J. Strid provided *Igh7*$^{-/-}$ mice. S.H. and F.A.R. provided experimental support. J.A.-L., M.V.F., M.F.V., A.D.-S., D.E.R., S.J.V., M.M.W. and G.E.B. reviewed data. J.A.-L., A.D.-S. and G.E.B. wrote and revised the manuscript. All other authors corrected and approved the final version of the manuscript. M.F.V. and P.J. contributed equally to this manuscript.

Competing interests The authors declare no competing interests.

Additional information

Supplementary information The online version contains supplementary material available at https://doi.org/10.1038/s41586-020-03118-2.

Correspondence and requests for materials should be addressed to G.E.B.

Peer review information *Nature* thanks Stuart Brierley, Magnus Simrén and the other, anonymous, reviewer(s) for their contribution to the peer review of this work. Peer reviewer reports are available.

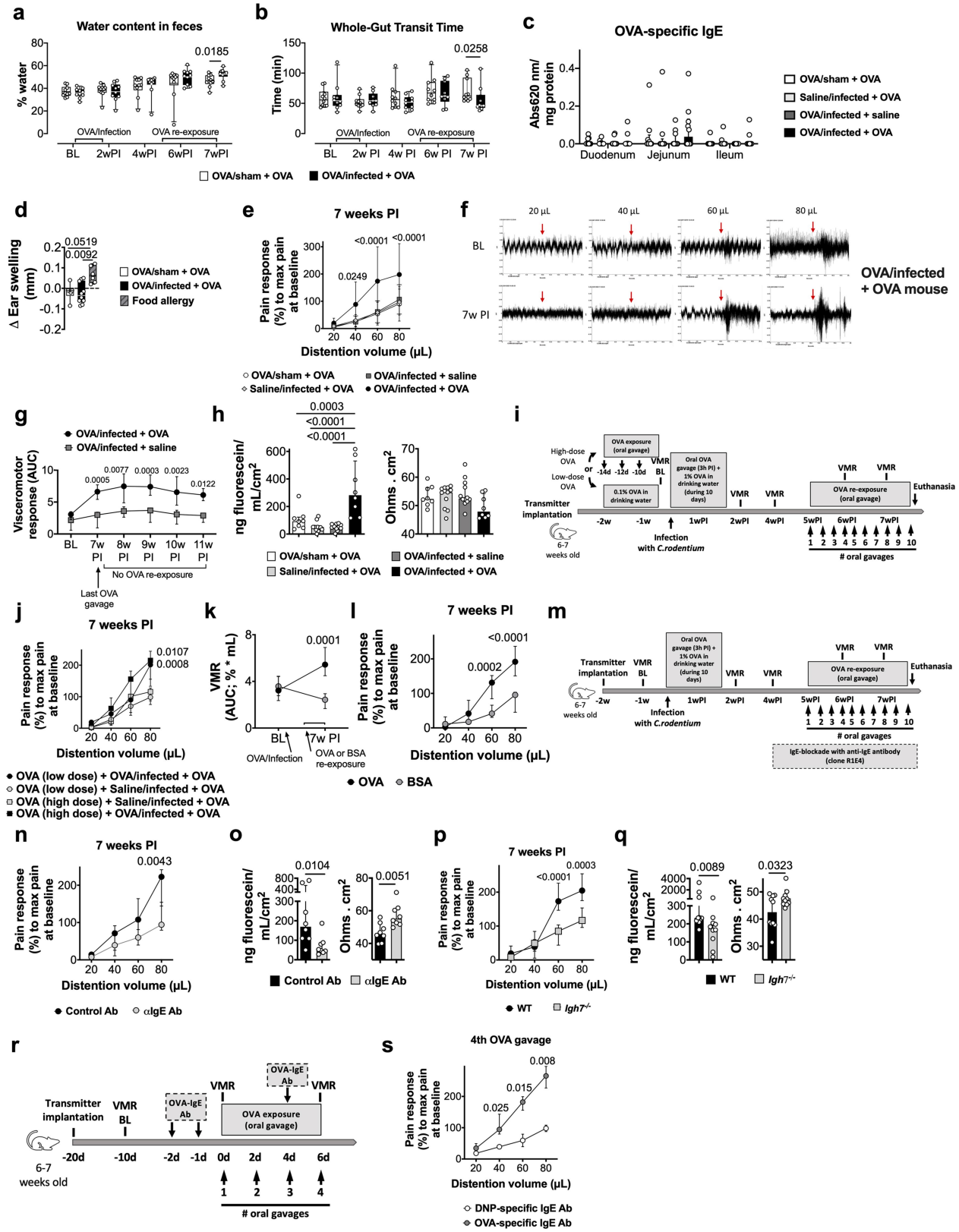

Extended Data Fig. 1 | See next page for caption.

Extended Data Fig. 1 | Extended analysis of the OVA-specific immune response and VHS in post-infectious mice. a, **b**, diarrhoea development quantification by (**a**) water content in faeces and (**b**) whole-gut transit time upon gavage of carmine red dye in OVA/sham + OVA, OVA/infected + OVA (n = 10/group) mice. **c**, quantification of OVA-specific IgE in intestinal homogenates of OVA/sham + OVA, saline/infected + OVA, OVA/infected + saline and OVA/infected + OVA mice (n = 9, 10, 10 and 9, respectively) at 7 weeks post-infection. **d**, ear-swelling after intradermal injection of OVA in OVA/sham + OVA (n = 6), OVA/infected + OVA (n = 10), at 7 weeks post-infection, and OVA-allergy mice (n = 6, 10 and 6, respectively). **e**, **f**, VMR to colorectal distention in (**e**) OVA/sham + OVA, OVA/infected + saline, saline/infected + OVA and OVA/infected + OVA mice (n = 12, 11, 11 and 13, respectively) and (**f**) tracing of a electromyographic response to 20-µL-, 40-µL-, 60-µL- and 80-µL-volume colorectal distention in a OVA/infected + OVA mouse at baseline and 7 weeks post-infection. **g**, VMR to colorectal distention in OVA/infected + OVA (n = 7) and OVA/infected = Saline (n = 7 and 5, respectively) mice at baseline (BL), 7 weeks post-infection (PI) and after 1, 2, 3 and 4 weeks after stopping oral OVA or saline re-exposure, respectively. **h**, colonic permeability in BALB/c mice expressed as passage of fluorescein sodium (left) and transepithelial resistance (right) in OVA/sham + OVA, saline/infected + OVA, OVA/infected + saline and OVA/infected + OVA mice (n = 8, 11, 12 and 8, respectively) at 7 weeks post-infection. **i**, scheme illustrating the post-infectious protocol with prior OVA tolerization. **j**, VMR to colorectal distention in mice OVA-tolerized (high-dose) + saline/infected + OVA, OVA-tolerized (high-dose) + OVA/infected + OVA, OVA-tolerized (low-dose) + saline/infected + OVA and OVA-tolerized (low-dose) + OVA/infected + OVA (n = 6, 9, 6 and 8, respectively). **k**, **l**, VMR to colorectal distention in mice OVA/infected repeatedly gavaged with BSA compared to OVA (n = 6 and 10, respectively). **m**, scheme illustrating the post-infectious protocol in mice treated with anti-IgE antibody. **n**, VMR to colorectal distention in OVA/infected + OVA mice treated with anti-IgE antibody or control antibody (n = 8/group). **o**, colonic permeability expressed as passage of fluorescein sodium (left) and transepithelial resistance (right) of (**l**) VHS mice treated with anti-IgE antibody or control antibody (n = 8/group). **p**, VMR to colorectal distention in OVA/infected + OVA mice with WT or Igh7$^{-/-}$ background (n = 10/group). **q**, colonic permeability expressed as passage of fluorescein sodium (left) and transepithelial resistance (right) of OVA/infected + OVA mice with *Igh7*$^{-/-}$ background or WT mice (n = 10/group) at 7 weeks post-infection. **r**, scheme illustrating the protocol in mice that received monoclonal OVA-specific IgE antibody. **s**, VMR to colorectal distention in naïve mice treated with monoclonal OVA-specific IgE antibody or monoclonal Dinitrophenyl (DNP) antibody (n = 7 and 6, respectively). Two-tailed Mann–Whitney test in **a** and **b** for every time point, and in **o** and **q** (left); two-tailed t-test for **q** (right). Kruskal–Wallis test (Dunn's multiple-comparisons test) in **c** and **d**. One-way ANOVA (Sidak's multiple-comparisons test) in **h**. Two-way repeated ANOVA (Sidak's multiple-comparisons test) in **e, g, j–l, n, p** and **s**. Data shown as Box-and-whiskers (centre line, median; box, 25th-75th percentiles; whiskers, 10th-90th percentiles) in **a**, **b** and **d** and median ± IQR in **c**, **e**, **g**, **h**, **j–l, n-q** and **s**. VMR, visceromotor response; BL, baseline; w, week; d; day.

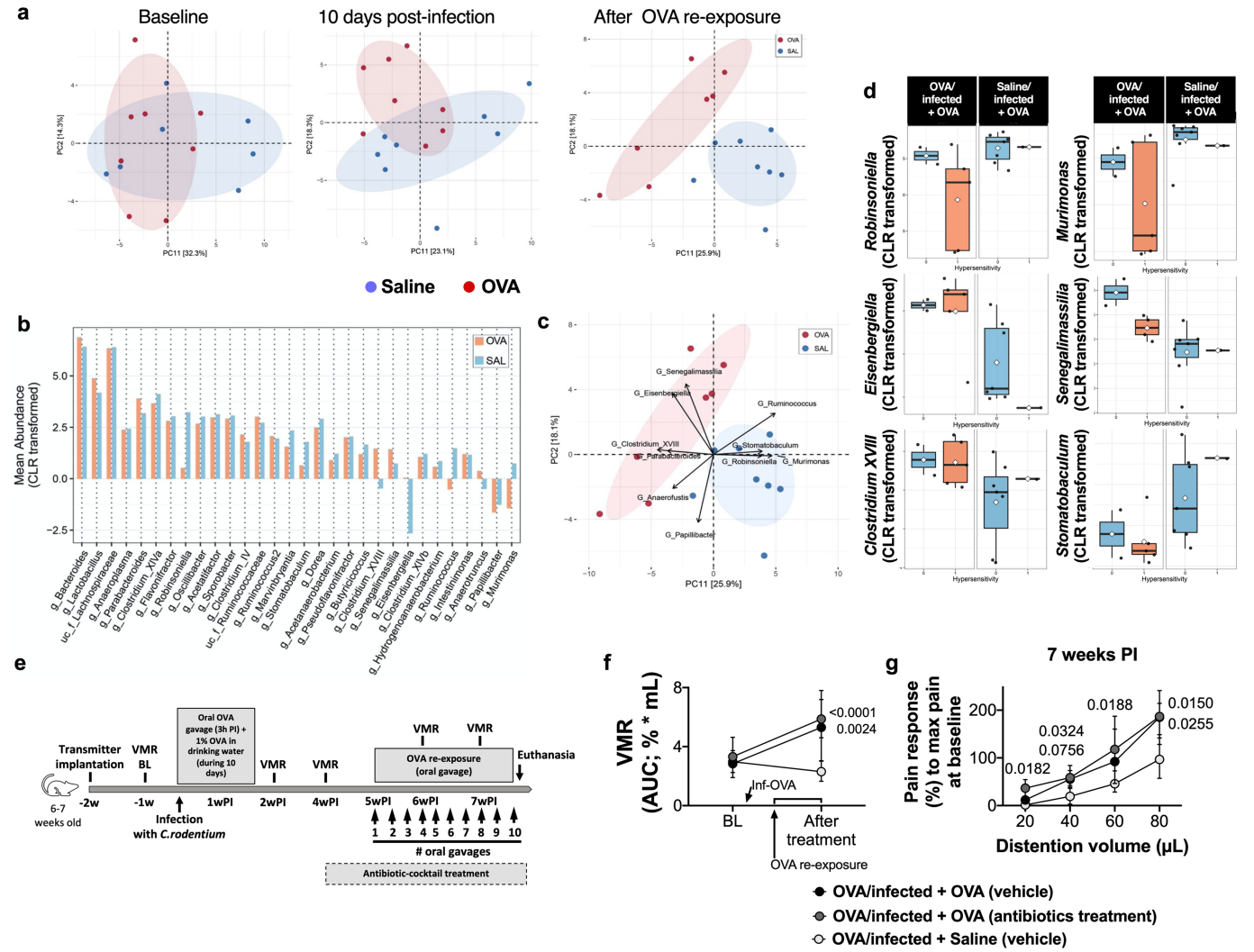

Extended Data Fig. 2 | Changes in microbiota composition are not likely to be associated with the development in VHS. a, changes in the gut microbiome composition over time studied by ordination (PCA) plot before the infection, 10 days after infection (R2 = 0.11, p-value = 0.02), and after OVA gavage (R2 = 0.18, p-value = 0.002) between OVA/infected and saline/infected (n = 8/group) mice. The numbers in brackets indicate the variation explained by each axis (PCA: principal component analysis). **b**–**d**, drivers of variation in the murine intestinal community after OVA re-exposure. **b**, Comparison of mean abundance of taxa between OVA- and saline-infected mice. Bacterial abundances were computed using centred log-ratio transformation (CLR; two-sided Mann–Whitney test, FDR <0.2). **c**, ordination biplot of PCA analysis showing the significant contributors in the community variation. Arrows indicate the relative importance of each genus (permutation-based P < 0.05). **d**, abundance of genus *Robinsoniella*, *Eisenbergiella*, *Senegalimassilia*, *Murimonas*, *Clostridium_XVIII* and *Stomatobaculum* by group and VHS (two-sided Mann–Whitney test, FDR >0.1). **e**, scheme illustrating the post-infectious protocol in mice treated with antibiotics. **f, g**, VMR to colorectal distention in VHS (OVA/infected + OVA) mice treated with antibiotics or control, and compared to OVA/infected + saline mice (n = 10, 7 and 6, respectively) (**g** depicts the VMM response at 7 weeks post-infection). In **d**, VHS threshold was established based on the 95th percentile of visceromotor responses at baseline (AUC >4.8). There was no significant association between VHS and bacterial abundance in any group (two-tailed Mann–Whitney test). X-axis indicates absence (0) and presence (1) of VHS. Two-way ANOVA 9(Sidak's multiple-comparisons test) in **f** and **g**. Data shown as box-and-whiskers ± 1.5 IQR in **d** and as median ± IQR in **f** and **g**. VMR, visceromotor response; BL, baseline; w, week.

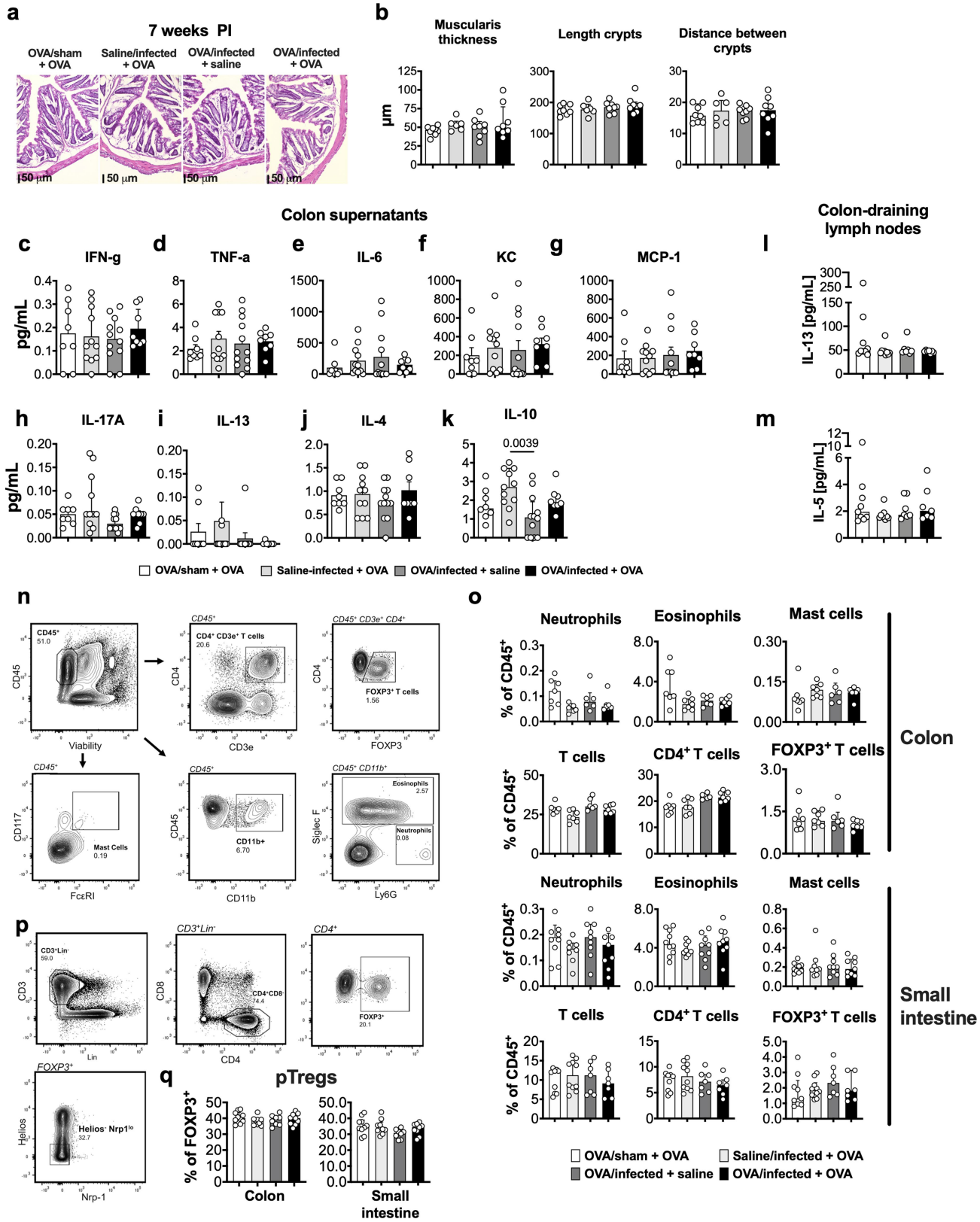

Extended Data Fig. 3 | See next page for caption.

Extended Data Fig. 3 | Analysis of 'low grade' inflammation in colonic samples of post-infectious mice. a, Representative H&E-stained colonic sections from OVA/sham + OVA, OVA/infected + saline, saline/infected + OVA and OVA/infected + OVA at 7 weeks post-infection. **b**, thickness of the colonic muscularis (left), length of the crypts (middle) and distance between crypts (right), measured in OVA/sham + OVA, saline/infected + OVA ($n = 6$), OVA/infected + saline and OVA/infected + OVA mice ($n = 8, 6, 8$ and 8, respectively) at 7 weeks post-infection. **c**–**k**, concentration of (**c**) IFN-γ, (**d**) TNF, (**e**) IL-6, (**f**) KC (murine IL-8 homologue), (**g**) MCP-1, (**h**) IL-17A, (**i**) IL-13, (**j**) IL-4 and (**k**) IL-10 assessed in colonic supernatant and (**l**) IL-13 and (**m**) IL-5 in colon-draining lymph nodes of OVA/sham + OVA, saline/infected + OVA, OVA/infected + saline and OVA/infected + OVA mice ($n = 8, 11, 12$ and 8, respectively, for **c**–**k**; $n = 7, 7, 9$ and 9, respectively for **l** and **m**). **n**–**q**, immune cell quantification along the intestinal tract: (**n** and **p**) gating strategy; (**o**) quantification of population of $CD11b^+Ly6G^+SiglecF^-$ neutrophils, $CD11b^+SiglecF^+$ eosinophils, $CD117^+FcR\varepsilon I^+$ mast cells, $CD3^+$ T cells, $CD3^+CD4^+$ T cells, $CD3^+CD4^+Foxp3^+$ T cells and (**q**) $Helios^-Nrp1^{lo}FOXP3^+$ pTregs in the colon and small intestine in OVA/sham + OVA, saline/infected + OVA, OVA/infected + saline and OVA/infected + OVA mice ($n = 7, 6, 7$ and 7, respectively, for **o** (colon); 9, 8, 9 and 10, respectively, for **o** (small intestine); 9, 9, 8 and 10, respectively, for **q** ($Helios^-Nrp1^{lo}FOXP3^+$ pTregs in colon); 9, 9, 8 and 10, respectively, for **q** ($Helios^-Nrp1^{lo}FOXP3^+$ pTregs in small intestine);. One-way ANOVA (Sidak's multiple-comparisons test) in **b**–**m**, **o** and **q**. Data shown median ± IQR in **b**–**m**, **o** and **q**.

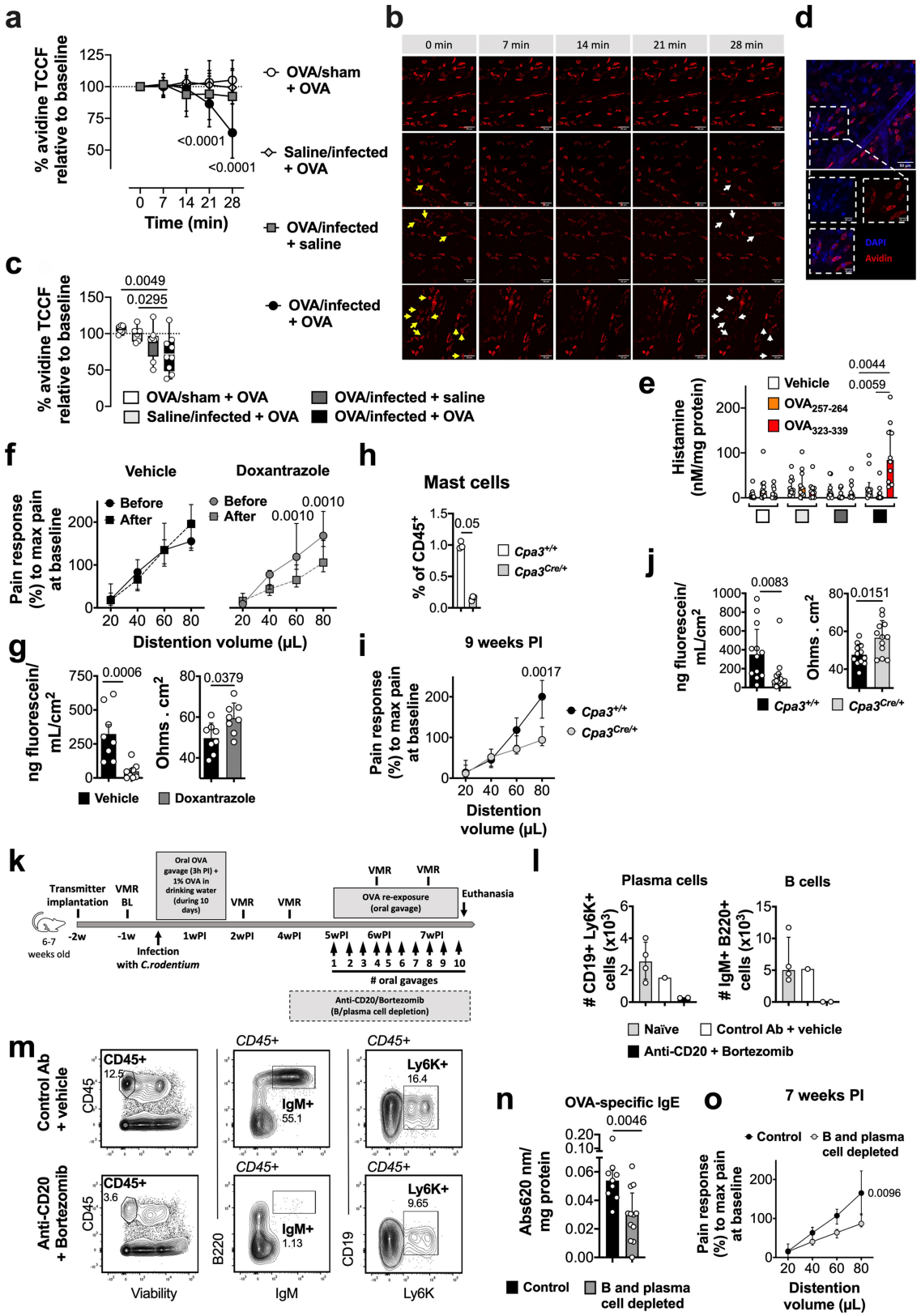

Extended Data Fig. 4 | See next page for caption.

Extended Data Fig. 4 | Extended analysis of mast cell activation as key players in the development of OVA-induced VHS in post-infectious mice. **a**–**c**, avidin-fluorescence intensity over time (expressed as TCCF) in MC from OVA/sham + OVA, saline/infected + OVA OVA/infected + saline and OVA/infected + OVA mice (n = 222 [7 mice], 145 [6 mice], 202 [8 mice] and 239 [9 mice], respectively), (**a**) shown as percentage at times = 0, 7, 14, 21 and 28 min, (**b**) micrographs and (**c**) shown at time = 28 min as median per mouse. In **b**, arrows point to representative MC showing degranulation (yellow, 28 min) compared to baseline (white, 0 min). **d**, representative image of double-staining using DAPI and avidin in fixed colonic tissue from healthy mice (n = 3). **e**, Histamine quantification in supernatant collected from OVA/sham + OVA, saline/infected + OVA, OVA/infected + saline and OVA/infected + OVA (n = 10/group) at 7 weeks post-infection. **f**, VMR to colorectal distention in OVA/infected + OVA mice (d) treated with doxantrazole or vehicle (n = 14 and 11, respectively). **g**, colonic permeability expressed as passage of fluorescein sodium (left) and transepithelial electrical resistance (right) of OVA/infected + OVA mice treated with doxantrazole or vehicle (n = 8/group) at 8 weeks post-infection. **h**, quantification of population of $CD117^+FcR\varepsilon I^+$ mast cells in intestinal lamina propria from $Cpa3^{Cre/+}$ and WT mice (n = 3/group). **i**, VMR to colorectal distention in OVA/infected + OVA mice with $Cpa3^{Cre/+}$ background or WT littermates (n = 13 and 12, respectively). **j**, colonic permeability expressed as passage of fluorescein sodium (left) and transepithelial electrical resistance (right) in OVA/infected + OVA mice with $Cpa3^{Cre/+}$ background or WT littermates (n = 12/group) at 9 weeks post-infection. **k**, scheme illustrating the post-infectious protocol in mice treated with anti-CD20 antibody and bortezomib. **l**, anti-CD20 (5D2 clone) antibody and bortezomib depleted $CD19^+$ $Ly6K^+$ plasma cells (left) and $B220^+$ IgM^+ B cells (right) from the colon of mice compared to control antibody/vehicle and naïve mice (n = 2, 1 and 4, respectively) and (**m**) gating strategy used to validate B cell and plasma cell depletion. **n**, quantification of OVA-specific IgE in colon samples homogenates from OVA/infected + OVA mice treated with anti-CD20 antibody and bortezomib or control antibody and vehicle (n = 12 and 9, respectively). **o**, VMR to colorectal distention in OVA/infected + OVA mice treated with anti-CD20 antibody/bortezomib or control antibody/vehicle (n = 3 and 4, respectively). Mixed-effects model (Dunnett's multiple-comparisons test) in **a** and **e**. One-way ANOVA (Sidak's multiple-comparisons test) in **c**. two-way repeated measures ANOVA (Sidak's multiple-comparisons test) in **f**, **(l)** and **o**. Two-tailed Mann–Whitney in **g, h, j** and **n**. Data are shown as median ± IQR in **a, e**–**j, l, n** and **o**, and box-and-whiskers (centre line, median; box, 25th and 75th percentiles; whiskers, 10th and 90th percentiles) in **c**. VMR, visceromotor response; BL, baseline; w, week.

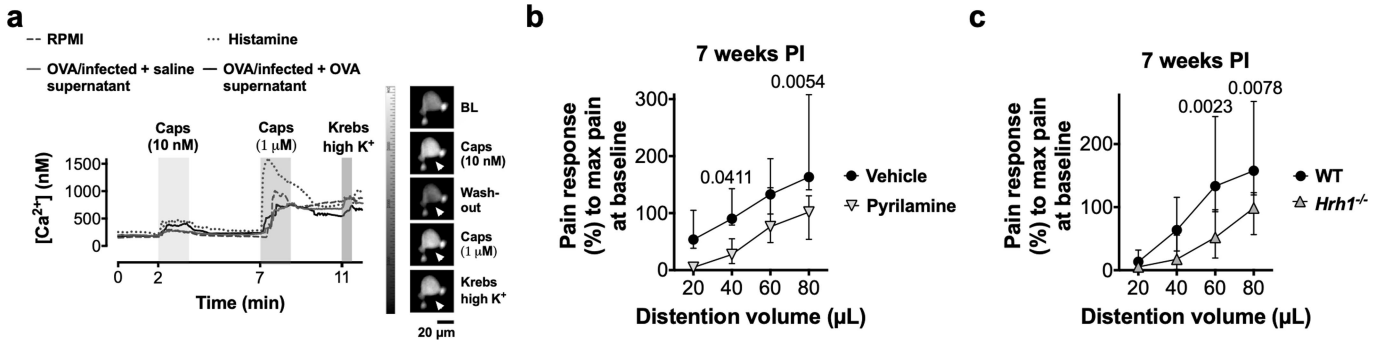

Extended Data Fig. 5 | H_1R mediates OVA-induced VHS in post-infectious mice. a, representative tracing and Fura-2 ratiometric fields of DRG neurons ($TRPV1^+$ neuron [right] indicated by arrowhead). **b, c**, VMR to colorectal distention in OVA/infected + OVA mice (**a**) treated with vehicle and pyrilamine ($n = 9$ and 8, respectively) and (**b**) with WT and $Hrh1^{-/-}$ background ($n = 13$ and 9, respectively). Two-way repeated measures ANOVA (Sidak's multiple-comparisons test) in **b** and **c**. Data are shown as median ± IQR.

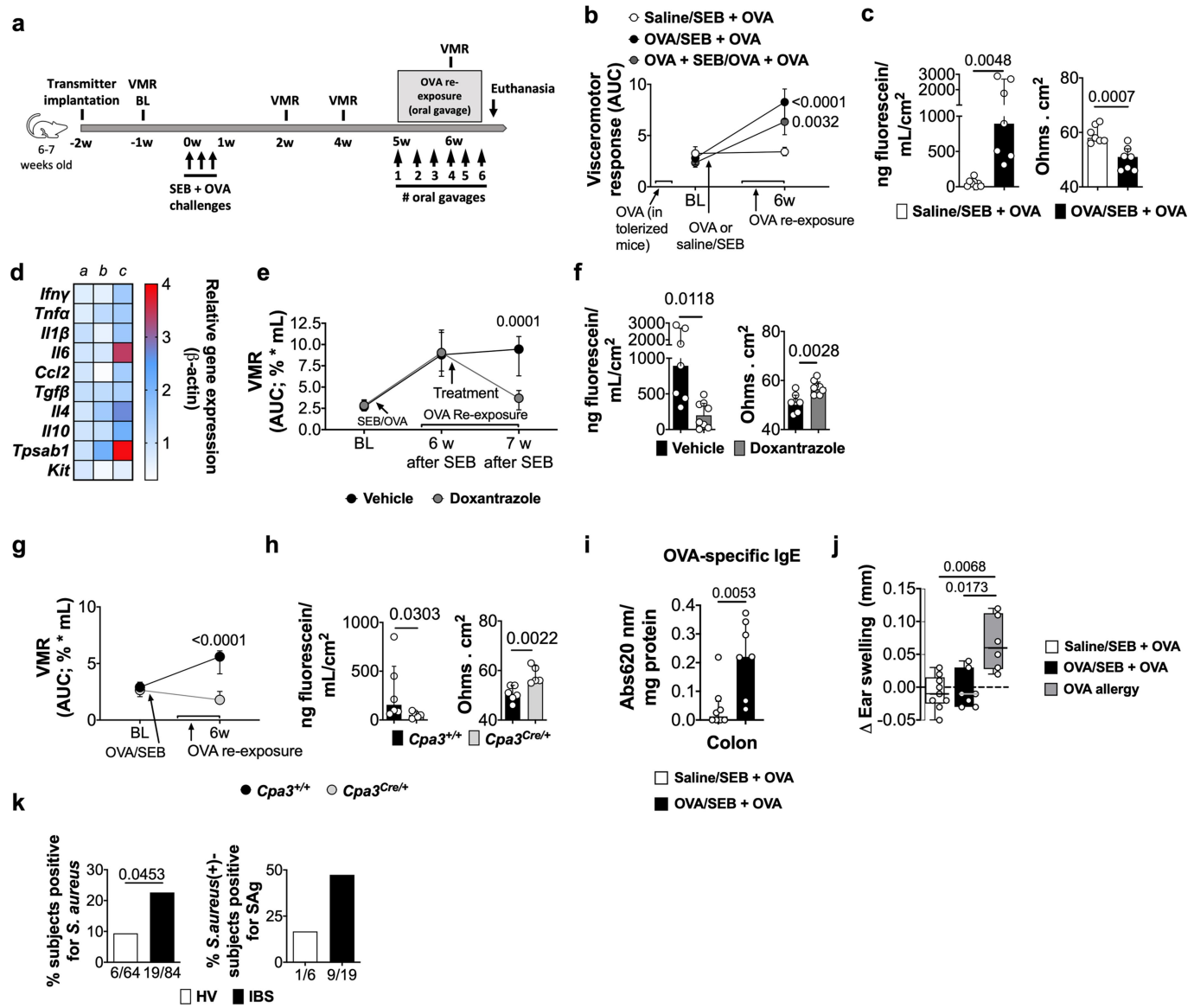

Extended Data Fig. 6 | SEB induces MC-mediated OVA-induced VHS upon comparable to *C. rodentium* infection. a, scheme illustrating the SEB protocol. **b**, VMR to colorectal distention in saline/SEB + OVA, OVA/SEB + OVA and OVA (low dose) + OVA/SEB + OVA mice ($n = 10$, 14 and 4, respectively). **c**, colonic permeability expressed as passage of fluorescein sodium (left) and transepithelial electrical resistance (right) of saline/SEB + OVA and OVA/SEB + OVA ($n = 8$ and 7, respectively) mice. **d**, heat-map of the gene expression of inflammatory genes and mast-cell-related genes in OVA/saline + OVA (*a*), saline/SEB + OVA (*b*) and OVA/SEB + OVA mice (*c*) ($n = 21$, 7 and 7, respectively; except for Tryptase α/β-1: $n = 7$/group). **e**, VMR to colorectal distention in SEB-VHS mice treated with doxantrazole or vehicle ($n = 8$ and 9, respectively). **f**, colonic permeability expressed as passage of fluorescein sodium (left) and transepithelial electrical resistance (right) of SEB-VHS mice treated with doxantrazole or vehicle ($n = 8$ and 7, respectively). **g**, VMR to colorectal distention in OVA/SEB + OVA mice with Cpa3Cre/+ background or WT littermates ($n = 5$ and 6, respectively). **h**, colonic permeability expressed as passage of fluorescein sodium (left) and transepithelial electrical resistance (right) of OVA/SEB + OVA mice with *Cpa3*$^{Cre/+}$ background or WT littermates ($n = 5$ and 6, respectively). **i**, quantification of OVA-specific IgE in colon homogenates of saline/SEB + OVA and OVA/SEB + OVA mice ($n = 8$ and 7, respectively). **j**, ear-swelling after intradermal injection of OVA in saline/SEB + OVA, OVA/SEB + OVA and OVA-allergy mice ($n = 9$, 7 and 6, respectively) mice. **k**, % of HV and IBS patients ($n = 64$ and 84, respectively) positive for *S. aureus* (left) and SAg-encoding *S. aureus* (right) in faecal samples. Numbers below the bars represent the ratio of positive and total HV and patients. Two-way repeated ANOVA (Sidak's multiple-comparisons test) in **b**, **e** and **g**. Two-tailed unpaired *t*-test in **c** and **f**. Two-tailed Mann–Whitney test in **h** and **i**. Kruskal–Wallis test (Dunn's multiple-comparisons test) in **d** and **j**. Two-sided Fisher's exact test in **k**. Data shown as median ± IQR in **b, e**–**i** and box-and-whiskers (centre line, median; box, 25th-75th percentiles; whiskers, 10th-90th percentiles) in **j**. VMR, visceromotor response; BL, baseline; w, week. In **d**, *Tpsab1*, *Il4*, *Il6* and *Il10* gene expression differences were statistically significant in OVA/SEB + OVA vs. OVA/saline + OVA (adjusted $P = 0.0005$, 0.0004, 0.0163 and 0.0039, respectively).

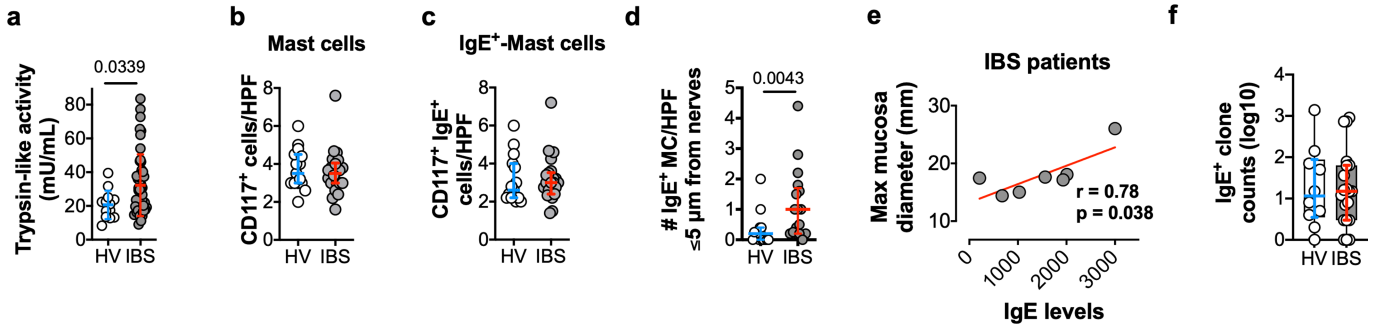

Extended Data Fig. 7 | Extended analysis of mast cells and IgE in human samples. a, measurement of trypsin-like activity in supernatants of rectal biopsies from HV and IBS patients ($n = 13$ and 48, respectively) in basal conditions. **b, c**, number of (**a**) MC ($CD117^+$) and (**b**) IgE^+-MC ($CD117^+$ IgE^+) quantified in mucosal rectal biopsies from HV and IBS patients ($n = 15$ and 22, respectively). **d**, quantification of $CD117^+$ IgE^+ cells (MC) at ≤ 5 µm from nerve fibres (β tubulin III^+ cells) in HV and IBS patients ($n = 15$ and 17, respectively). **e**, correlation between the IgE TCCF and max mucosal diameter after food-antigen injection in IBS patients ($n = 7$). **f**, number of IgE^+ clones was quantified in mucosal rectal biopsies cDNA from HV and IBS patients ($n = 10$ and 20, respectively) using deep sequencing. Two-tailed Mann–Whitney test in **a**–**d** and **f**. two-tailed Pearson's correlation in **e**. Data are shown as median ± IQR in **a**–**d**, and as box-and-whiskers (centre line, median; box, 25th and 75th percentiles; whiskers, 10th and 90th percentiles) in **f**. HPF = high power field.

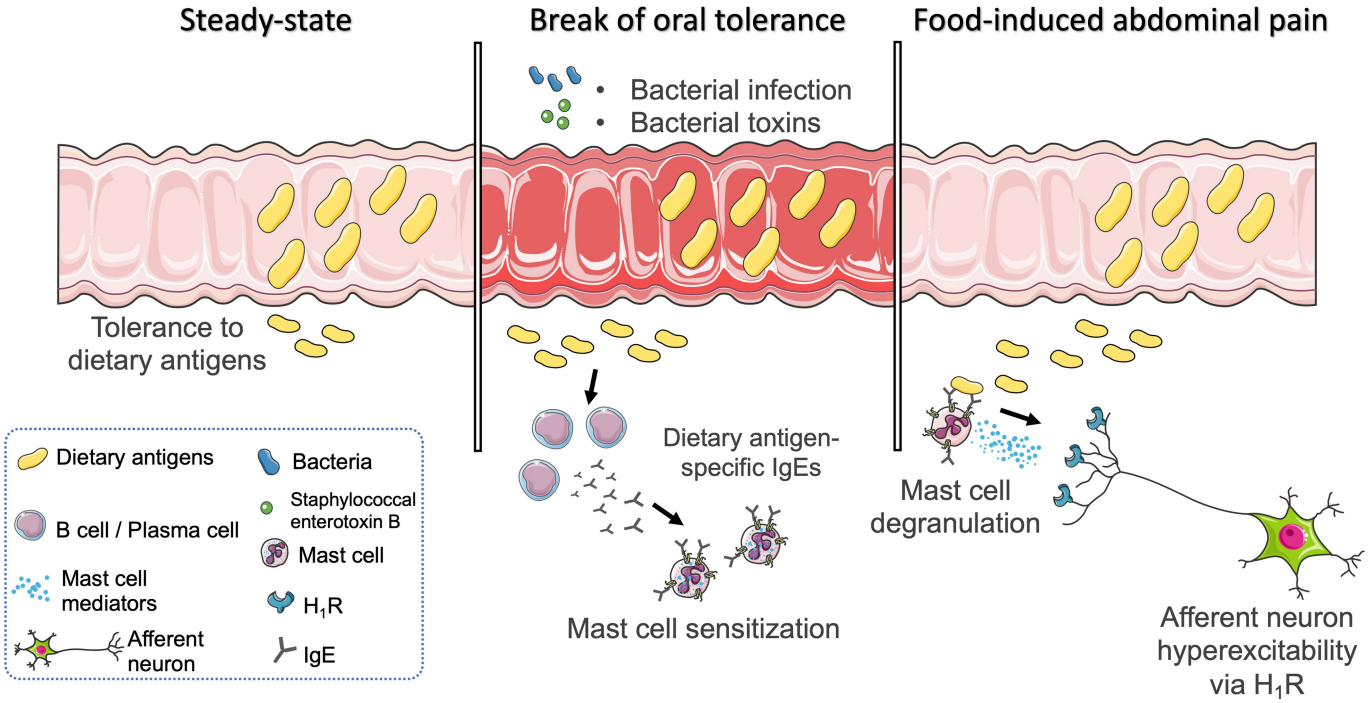

Extended Data Fig. 8 | Graphical representation of the mechanism proposed: local immune response to dietary antigens triggered by bacterial infection leads to food-induced abdominal pain. Bacterial infection (or bacterial toxins, SEB) can trigger break of oral tolerance to food antigens leading to food-induced VHS upon food-antigen re-exposure. OVA-specific IgE antibodies bind to and sensitizes tissue-resident mast cells, which are activated upon re-exposure to OVA during feeding and release mediators that sensitize afferent neurons via H_1R-mediated pathway. Components of this figure were created using Servier Medical Art templates, which are licensed under a Creative Commons Attribution 3.0 Unported License; https://smart.servier.com.

Extended Data Table 1 | Colonic compliance (volume-pressure relationship) evaluated in animals subjected to VMR recordings

Group	Genotype / Treatment	Strain	Volume												Weeks post-infection / post SEB-administration / post-WAS
			20 µL			40 µL			60 µL			80 µL			
			Mean (mmHg)	SD	Significance compared to control	Mean (mmHg)	SD	Significance compared to control	Mean (mmHg)	SD	Significance compared to control	Mean (mmHg)	SD	Significance compared to control	
OVA/control + OVA	WT	BALB/c	24.23	5.36	-	40.74	8.35	-	55.02	9.54	-	71.74	10.72	-	7
OVA/infected + OVA	WT	BALB/c	22.74	3.85	ns	38.35	5.92	ns	53.52	8.47	ns	70.03	8.80	ns	7
OVA/infected + saline	WT	BALB/c	21.14	3.70	ns	37.69	7.87	ns	48.39	12.72	ns	63.16	15.70	ns	7
Saline/infected + OVA	WT	BALB/c	23.49	3.26	ns	39.76	4.91	ns	53.54	5.66	ns	71.63	9.03	ns	7
OVA/infected + BSA	WT	BALB/c	22.05	4.61	ns	40.42	7.64	ns	56.99	9.15	ns	76.48	10.32	ns	7
OVA (low) + saline/infected + OVA	WT	BALB/c	26.59	7.02	-	47.35	10.31	-	60.60	11.11	-	79.23	13.13	-	7
OVA (low) + OVA/infected + OVA	WT	BALB/c	22.71	4.29	ns	44.34	5.89	ns	59.29	7.00	ns	75.31	7.40	ns	7
OVA (high) + saline/infected + OVA	WT	BALB/c	27.12	6.45	-	47.88	9.26	-	61.13	10.56	-	79.77	12.57	-	7
OVA (high) + OVA/infected + OVA	WT	BALB/c	23.56	4.95	ns	45.19	6.11	ns	60.14	7.62	ns	76.16	8.16	ns	7
OVA/infected + OVA	WT / Vehicle	BALB/c	23.77	4.29	-	45.94	5.61	-	61.47	7.09	-	79.49	10.81	-	7
OVA/infected + OVA	WT / antibiotic-cocktail	BALB/c	23.24	4.57	ns	43.87	4.93	ns	55.99	5.59	ns	74.75	2.88	ns	7
OVA/infected + OVA	WT / Vehicle	BALB/c	25.11	1.61	-	40.35	1.76	-	54.97	4.84	-	70.63	7.73	-	8
OVA/infected + OVA	WT / Doxantrazole	BALB/c	17.19	1.12	ns	32.28	2.21	ns	49.26	4.55	ns	66.88	3.35	ns	8
OVA/infected + OVA	*Cpa3* $^{+/+}$	BALB/c	26.86	5.79	-	43.89	12.02	-	60.70	15.08	-	78.63	16.41	-	9
OVA/infected + OVA	*Cpa3* $^{Cre/+}$	BALB/c	21.18	5.25	ns	39.95	7.10	ns	51.67	6.24	ns	64.92	5.69	ns	9
OVA/infected + OVA	WT / Vehicle	BALB/c	22.73	1.51	-	40.32	3.36	-	56.51	7.38	-	67.76	9.45	-	7
OVA/infected + OVA	WT / antiCD-20 + Bortezomib	BALB/c	23.95	4.15	ns	40.34	13.09	ns	53.73	19.77	ns	67.48	23.61	ns	7
OVA/infected + OVA	WT / isotype control antibody	BALB/c	21.22	4.64	-	40.06	9.06	-	50.82	11.35	-	64.83	14.84	-	7
OVA/infected + OVA	WT / αIgE antibody	BALB/c	24.78	5.03	ns	40.69	4.62	ns	54.58	8.33	ns	67.02	13.27	ns	7
OVA/infected + OVA	WT	BALB/c	16.06	3.74	-	42.49	12.39	-	58.23	9.98	-	74.62	10.23	-	7
OVA/infected + OVA	*Igh* KO	BALB/c	19.62	6.11	ns	36.95	5.33	ns	54.50	6.86	ns	**74.47**	5.45	ns	7
Naïve	DNP-specific IgE antibody	BALB/c	19.71	3.52	-	35.87	7.18	-	53.58	6.48	-	72.98	8.25	-	*After last OVA challenge
Naïve	OVA-specific IgE antibody	BALB/c	17.78	5.75	ns	38.69	6.80	ns	56.06	6.69	ns	78.13	5.53	ns	*After last OVA challenge
OVA/infected + OVA	WT / Vehicle	BALB/c	25.25	1.67	-	43.77	4.10	-	56.32	10.54	-	70.37	10.68	-	7
OVA/infected + OVA	WT / Pyrilamine	BALB/c	21.97	3.00	ns	39.95	5.81	ns	58.44	7.26	ns	70.88	4.49	ns	7
OVA/infected + OVA	WT	BALB/c	26.41	5.08	-	42.67	6.71	-	56.46	7.26	-	74.55	9.70	-	7
OVA/infected + OVA	*Hrh1* KO	BALB/c	23.58	6.71	ns	41.94	9.55	ns	58.51	11.71	ns	78.01	12.91	ns	7
Saline/SEB + OVA	WT	BALB/c	26.88	3.35	-	43.39	6.12	-	57.66	7.78	-	74.39	8.93	-	7
OVA/SEB + OVA	WT	BALB/c	23.14	3.83	ns	39.70	7.41	ns	50.40	12.14	ns	72.17	14.31	ns	7
OVA/SEB + OVA	WT / Doxantrazole	BALB/c	23.86	5.80	ns	38.73	9.35	ns	53.17	12.86	ns	68.93	15.71	ns	8
OVA/SEB + OVA	*Cpa3* $^{+/+}$	BALB/c	25.10	3.57	-	44.37	7.07	-	53.78	5.10	-	64.63	10.33	-	7
OVA/SEB + OVA	*Cpa3* $^{Cre/+}$	BALB/c	24.75	7.69	ns	39.70	12.39	ns	54.87	11.99	ns	68.16	16.28	ns	7

ns, non-significant.

Extended Data Table 2 | Demographic data and characteristics of IBS patients participating in food-antigen injection protocol

Patient	IBS subtype	Post-infectious IBS	Gender	Age (years)	Symptom severity (VAS pain score)	Associated psychological distress	Food antigen-specific IgE				Symptom development (time food intake)	Reported relationship between food intake and symptom generation	Reported food items associated with positive mucosal edema reaction
							Soy	Wheat	Gluten	Milk			
IBS 1	IBS-D	No	M	27	5	Yes	n.d.	n.d.	n.d.	n.d.	5-6 h	Diarrhea, abdominal pain, bloating	-
IBS 2	IBS-U	No	F	48	4	No	n.d.	n.d.	n.d.	n.d.	30 min - 1 day	Diarrhea, abdominal pain, abdominal cramps, belching	-
IBS 3	IBS-M	No	F	25	6	Yes	n.d.	n.d.	n.d.	n.d.	1-3 h	Diarrhea, abdominal cramps, bloating	Gluten
IBS 4	IBS-D	No	F	19	6	Yes	n.d.	n.d.	n.d.	n.d.	Immediately	Diarrhea, abdominal pain, abdominal cramps	Soy, milk
IBS 5	IBS-D	No	M	41	2	No	n.d.	n.d.	n.d.	n.d.	3h	Abdominal cramps	Wheat, gluten
IBS 6	IBS-D	No	F	19	5	Yes	n.d.	n.d.	n.d.	n.d.	Immediately - 6 h	Diarrhea, abdominal pain, abdominal cramps, flatulence	Wheat, gluten, milk
IBS 7	IBS-D	No	F	20	5	Yes	n.d.	n.d.	n.d.	n.d.	30 min - 3 h	Abdominal pain, abdominal cramps, bloating	Wheat, gluten, milk
IBS 8	IBS-D	No	F	50	6	Yes	n.d.	n.d.	n.d.	n.d.	30 min - 4 h	Abdominal pain	Milk
IBS 9	IBS-D	Yes	M	33	4	Yes	n.d.	n.d.	n.d.	n.d.	3h	Diarrhea, abdominal cramps, flatulence, bloating	-
IBS 10	IBS-D	Yes	M	31	10	No	n.d.	n.d.	n.d.	n.d.	10 min	Abdominal pain, flatulence	-
IBS 11	IBS-D	No	F	28	9	Yes	n.d.	n.d.	n.d.	n.d.	30 min	Diarrhea, abdominal pain	-
IBS 12	IBS-D	No	F	34	6	Yes	n.d.	n.d.	n.d.	n.d.	30 min - 1 h	Diarrhea, abdominal cramps, bloating, flatulence	Soy, wheat, milk
Median	-	-	8F / 4M	29, IQR [21-39]	5.5, IQR [4.25-6]	-	-	-	-	-	30min - 3h	-	-

M, male; F, female; IBS-D, IBS diarrhoea-predominant; IBS-U, IBS unsubtyped; IBS-M, IBS mixed bowel pattern; n.d., non-detected.

nature research

Corresponding author(s): Guy E. Boeckxstaens

Last updated by author(s): Nov 16, 2020

Reporting Summary

Nature Research wishes to improve the reproducibility of the work that we publish. This form provides structure for consistency and transparency in reporting. For further information on Nature Research policies, see Authors & Referees and the Editorial Policy Checklist.

Statistics

For all statistical analyses, confirm that the following items are present in the figure legend, table legend, main text, or Methods section.

n/a	Confirmed	
☐	☒	The exact sample size (*n*) for each experimental group/condition, given as a discrete number and unit of measurement
☐	☒	A statement on whether measurements were taken from distinct samples or whether the same sample was measured repeatedly
☐	☒	The statistical test(s) used AND whether they are one- or two-sided *Only common tests should be described solely by name; describe more complex techniques in the Methods section.*
☒	☐	A description of all covariates tested
☐	☒	A description of any assumptions or corrections, such as tests of normality and adjustment for multiple comparisons
☐	☒	A full description of the statistical parameters including central tendency (e.g. means) or other basic estimates (e.g. regression coefficient) AND variation (e.g. standard deviation) or associated estimates of uncertainty (e.g. confidence intervals)
☐	☒	For null hypothesis testing, the test statistic (e.g. *F*, *t*, *r*) with confidence intervals, effect sizes, degrees of freedom and *P* value noted *Give P values as exact values whenever suitable.*
☒	☐	For Bayesian analysis, information on the choice of priors and Markov chain Monte Carlo settings
☒	☐	For hierarchical and complex designs, identification of the appropriate level for tests and full reporting of outcomes
☐	☒	Estimates of effect sizes (e.g. Cohen's *d*, Pearson's *r*), indicating how they were calculated

Our web collection on statistics for biologists contains articles on many of the points above.

Software and code

Policy information about availability of computer code

Data collection	Visceromotor responses recordings were eanalyzed using Acknowledge 3.2.6 software. Afferent nerve recordings were analyzed using Spike2 software (V.607). Transepithelial resistance was analyzed using Clamp software (v9.00). For analysis of inflammatory cytokines in colonic supernatants FCAP Array Software (v3.0) was used. Flow cytometry analysis were performed using FlowJo software (V.10.0.8, Tree Star Inc.). Patch-clamp experiments were analyzed using pClamp 10.5 software (Molecular Devices). Ca2+ experiments were analyzed with TILLVision software (v4.5.66 build 10002; TILL Photonics). Immunostainings images were captured using Zen Black 2.3 SP1 software and processed with ImageJ 2.0.0-rc-54/1.52d. Live mast cell degranulation experiments were analyzed using Zen v14.0.20.201. For microbiome analysis, R (version 3.4.1) was used. Ordination analysis (PCA) with contributing bacteria was performed at genus-level using the vegan R package (functions: prcomp and envfit). Spot-forming cells in ELISPOT experiment were quantified with ImmunoSpot software (v7.0).
Data analysis	Data were plotted and statistical analysis were performed using GraphPad Prism software version 9 (9.0.0). Microbiome analysis was performed in R (version 3.4.1). Microbiome fastq sequences were demultiplexed using LotuS 1.565, then were further processed following the DADA2 microbiome pipeline (references in the methods). CoDaSeq R package function codaSeq.clr was used to transform bacterial abundances to control the compositionality of the sequencing data. Ordination analysis (PCA) with contributing bacteria was performed at genus-level using the vegan package (functions: prcomp and envfit; reference in the methods).

For manuscripts utilizing custom algorithms or software that are central to the research but not yet described in published literature, software must be made available to editors/reviewers. We strongly encourage code deposition in a community repository (e.g. GitHub). See the Nature Research guidelines for submitting code & software for further information.

Data

Policy information about availability of data

All manuscripts must include a data availability statement. This statement should provide the following information, where applicable:

- Accession codes, unique identifiers, or web links for publicly available datasets
- A list of figures that have associated raw data
- A description of any restrictions on data availability

The data for 16S rRNA gene sequences are available from the European Nucleotide Archive (https://www.ebi.ac.uk/ena/) at accession number PRJEB41204. All other relevant data generated and analyzed during the current study are available upon reasonable request to the corresponding author (GEB). Source data are provided with this paper.

Field-specific reporting

Please select the one below that is the best fit for your research. If you are not sure, read the appropriate sections before making your selection.

☒ Life sciences ☐ Behavioural & social sciences ☐ Ecological, evolutionary & environmental sciences

For a reference copy of the document with all sections, see nature.com/documents/nr-reporting-summary-flat.pdf

Life sciences study design

All studies must disclose on these points even when the disclosure is negative.

Sample size	For animal studies, the number of mice was selected based on power calculations performed based on previous or present studies carried out in our laboratory and in the field. For the assessment of the diarrhea-score, whole total transit time and water content in fecal water we used between 6 and 10 mice per experimental group. For measurement visceromotor response we used between 3 and 13 mice per experimental group/genotype/pharmacological treatment. For ELISpot assay, we used 4 mice per experimental group. For recording of afferent nerves experiment we used between 6 and 8 mice per experimental group. For measurement of colonic permeability, we used between 5 and 12 mice per group/genotype/pharmacological treatment. For analysis of gut microbiota, we used 8 mice per experimental group. For histology studies we used between 6 and 8 mice per experimental group. For measurement of cytokine levels, we used between 8 and 12 mice per experimental group. For measurement of gene expression in colonic murine samples we used between 5 and 21 mice per experimental group. For FACS analysis we used between 6 and 10 mice per experimental group. For measurement of OVA-specific immunoglobulins we used between 6 and 10 mice per experimental group in serum samples; and between 4 and 19 mice per experimental group in colonic samples. For evaluation of live MC degranulation, 145-239 MC were analyzed per group, from tissue isolated from 6-9 different mice/group. For evaluation of ear-swelling upon OVA intradermal injection we used between 6 and 10 mice per experimental group. For patch-clamp experiments in DRG neurons we used between 18 and 24 neurons per experimental group/pharmacological treatment. For measurement of Ca2+ responses we used between 51 and 126 neurons per group/genotype/pharmacological treatment. In human studies, no power calculations were performed. For the food-antigens injection study and the amount of participant was chosen based on a previous similar study performed in patients with eosinophilic esophagitis (Warners, M. J. et al. Gastroenterology. 2018): 8 HV subjects and 12 IBS patients were used. For the measurement of trypsin-like-activity, samples from the food antigens-injection sites of 8 IBS patients were processed, and 13 HV vs 48 IBS patients were compared at basal conditions. The number of samples evaluated was based in the number of IBS patients recruited for the food-antigen injection (4 of them could not be evaluated). For the measurement of trypsin-like-activity in basal conditions, we based the number in previous literature (Rolland-Fourcade C, et al., Gut 2017; Cenac N, et al. J Clin Invest. 2007). For assessment of IgE immunofluorescence, mucosal biopsies from 15 HV and 22 IBS patients were used, and for distance between IgE + mast cells and nerves, mucosal biopsies from, 15 HV and 17 IBS patients were used. The number of subjects evaluated here was chosen based on previous studies evaluating distance between MC and nerve fibers in IBS patients and HV (Barbara G. et al., Gastroenterology 2004). For bacteria (S. aureus and S. pyogenes) and SAgs, the number of samples was chosen based on a previous study performed in healthy subjects where the presence of S. aureus was evaluated (Benito D, et al., Microb Ecol. 2013): 64 HV subjects and 84 IBS patients were used. For IgH sequence analysis, the number of samples was chosen based in literature (Nielsen SCA, et al., Sci Transl Med. 2019).
Data exclusions	In the food-antigen injection study, the reaction to saline in one IBS patient and the reaction to soy in one HV were excluded because 2 and 3 injections were needed to inoculate the sample, respectively. Exclusion based on this criteria was determined prior the start of the study.
Replication	For visceromotor response recording (except mice receiving repeated BSA by oral gavage, B and plasma cell depletion, treatment with anti-IgE antibody and IgE-deficient mice and treatment with OVA-specific IgE), experiments were performed twice or more times and data from individual mice were pooled from all experiments. All attempts in replication were successful. Diarrhea score, WGTT and water content where performed in different batches of animals. WGTT and fecal water content confirmed results in diarrhea score. Similar number of mice were used per experiment duplicated for control group/treatment and experimental group. For afferent nerve recording and Ussing chambers, experiments were performed twice and data from individual mice were pooled from all experiments. All attempts in replication were successful. Similar number of mice were used per experiment duplicated for control group/treatment and experimental group. All in vivo and ex vivo experiments were routinely assessed on different days, including every group tested in each day. For FACS analysis, at least 2 experiments were performed for each tissue. The replication experiments were all successful. For experiments with cultures of DRG neurons, multiple biological replicates were used for each group. For Ca2+ experiments (except for Hrh1-/- DRG neurons), experiments were performed twice and neuron Ca2+ responses were pooled. All attempts in replication were successful. For experiments with live MC degranulation and histamine release, experiments were performed twice and data were pooled. The replication experiment was successful. For experiments involving human, in the assessment of IgE immunofluorescence and distance between IgE+ MC and nerves, stainings were performed in 2 to 4 days each experiment. Data from all experiments were pooled. For the food antigen injection, subjects were assessed in

groups of 2 to 3 per day, and data were pooled. For the measurement of trypsin-like-activity, experiments were performed at least twice. Replication was successful. For IgH sequence analysis, a single evaluation was performed including all samples.

Randomization

For experiments involving transgenic mice and pharmacological treatments, genetically modified mice and WT littermates or drug-treated- and vehicle/control-treated-mice were placed together in the same cages. Allocation was random. This held true for all experiments except IgE-deficient and Hrhr1 mice, where animals transgenic animals were placed in the same cage, and WT phenotype in separete cages. For pharmacological treatments, the online tool of GraphPad software (QuickCalcs) was used to randomly assign subjects to groups for treatment or vehicle/control.

Blinding

For pharmacological treatments and experiments with KO mice, the experimenter recording visceromotor responses was blinded for the treatment and control/vehicle or the mouse genotype and was unblinded after the analysis. For the afferent nerve recording experiment, the experimenter was blinded for the animal groups and was unblinded after the analysis. For the experiments involving cultures of DRG neuron, the experimenters were blinded after the analysis. For experiments involving microbiota analysis the experimenter was blinded for the analysis. For experiments involving live mast cell degranulation, the experimenter was blinded during the performance of the experiment and for the analysis of images, and was unblinded after the analysis.
For human experiments, the experimenters analyzing the reactions to food-antigens were blinded for the images/videos analyses and were unblinded after the analysis.
For histopathology assessment murine samples and immunostainings in human samples, five to ten images per sections were randomly captured and analyzed by the experimenter in a blinded manner. Experimenter was unblinded after the analysis.
For the analysis of immunoglobulin genes from tissue cDNA (IgE+ clones), the experimenter analyzing the number of clones was only unblinded after the analysis.

Reporting for specific materials, systems and methods

We require information from authors about some types of materials, experimental systems and methods used in many studies. Here, indicate whether each material, system or method listed is relevant to your study. If you are not sure if a list item applies to your research, read the appropriate section before selecting a response.

Materials & experimental systems

n/a	Involved in the study
☐	☒ Antibodies
☒	☐ Eukaryotic cell lines
☒	☐ Palaeontology
☐	☒ Animals and other organisms
☐	☒ Human research participants
☒	☐ Clinical data

Methods

n/a	Involved in the study
☒	☐ ChIP-seq
☐	☒ Flow cytometry
☒	☐ MRI-based neuroimaging

Antibodies

Antibodies used

For in vivo treatments, the B cell depleting antibody, IgG2a anti-CD20 (clone 5D2, isotype IgG2a, generously provided by Genentech), its control antibody (clone 3E5, isotype IgG2a, generously provided by Genentech) were administered i.p. (8 mg/kg). Anti-IgE antibody (clone R1E4; Catalog # EVC003; Kerafast) and its control antibody were administered i.p. (1 mg/kg). Mouse anti-OVA monoclonal IgE antibody (clone E-C1; Catalog # 7091; Chondrex) was adiministered i.p. (10 µg/mouse). Monoclonal Anti-Dinitrophenyl (DNP) antibody (clone SPE-7, Catalog #: D8406; Sigma) was administered i.p. (10 µg/mouse).

For FACS analysis, antibodies used for staining included:
Anti-CD45, APC-eFluor® 780, clone 30-F11 eBioscience 47-0451-82
Anti-Cd11b, PE-Cy7, clone M1/70 BD Biosciences 552850
Anti-Ly6G, PerCP-Cy5.5, clone 1A8 BD Biosciences 560602
Anti-SiglecF, PE, clone E50-2440 BD Biosciences 562068
Anti-FceRI, PE, clone MAR-1 eBioscience 12-5898-82
Anti-CD117, APC, clone 2B8 BD Biosciences 553356
Anti-CD49b, PerCP-eFluor® 710, clone DX5 eBioscience 46-5971-82
Anti-CD4, APC, clone RM4-5 eBioscience 17-0042-82
Anti-CD3e, PerCP-Cy5.5, clone 145-2C11 BD Biosciences 551163
Anti-FoxP3, PE, clone FJK-16s eBioscience 12-5773-82
Anti-B220, PE-Cy7, RA3-6B2 eBioscience 25-0452-82
Anti-IgM, FITC, clone II/41 eBioscience 11-5790-81
Anti-CD19, APC, clone 1D3 eBioscience 17-0193-82
Anti-Ly6K, PE, clone B33fc8k eBioscience 12-5929-82
Anti-CD8a, APC-Cy7, clone 53-6.7 BioLegend 100714
Anti-Nrp-1, PE, clone 761705 R&D FAB5994P
Anti-Cd11b, PE-Cy5, clone M1/70 Biolegend 101210
Anti-CD19, PE-Cy5, clone 1D3 eBioscience 15-0193-82
Anti-CD25, PerCP-Cy5.5, clone PC61 BioLegend 102030
Anti-CD44, AlexaFluor 700, clone IM7 BioLegend 103026
Anti-CD8a, APC-Cy7, clone 53-6.7 BioLegend 100714
Anti-Gata3, AlexaFluor 488, clone TWAJ eBioscience 53-9966-42
Anti NK-1.1, PE-Cy5, clone PK136 BioLegend 108716

Anti Helios, APC, clone 22F6 BioLegend 137222
Anti-CD3, eFluor450, clone 17A2 eBioscience 48-0032-82
Anti-FoxP3, PE-Cy7, clone FJK-16s eBioscience 25-5773-82

For immunostainings, the following primary antibodies were used: rabbit anti-human CD117, clone K963, 1:500 (catalog #: CD11718; Sanbio B.V.), mouse anti-human IgE, clone MHE-18, 1:250 (catalog #: 325502; BioLegend) and for nerve fibers chicken anti-beta III tubulin (catalog #: ab78078; Abcam). Then, secondary antibodies (Jackson ImmunoResearch) included Cy3 donkey anti-rabbit (1:500; catalog #: 711-165-152), Cy5 donkey anti-mouse (1:500; catalog #: 715-175-150) [for immunofluorescence intensity evaluation] and Cy3 donkey anti-chicken (1:300; catalog #: 703-165-155), Cy5 donkey anti-rabbit (1:500; catalog #: 711-175-152), A488 donkey anti mouse (1:500; catalog #: 715-545-150) [for distance evaluation between IgE+ mast cells and nerve fibers].

For ELISA experiments, Biotin Rat anti-Mouse IgE, 4µg/mL, (Catalog #: 553419, BD) Biosciences was used.

Validation

For the experiment of B cell depletion, the effectiveness of IgG2a anti-CD20 to deplete B cells was assessed in a pilot study (Supplementary Fig. 3a, b).
For the blocking of the interaction between IgE and FcεRI with the anti-IgE antibody (clone R1E4), the work of Smith CE et al (Proc Natl Acad Sci U S A. 2005) was used as a reference. No in-house validation was performed.

FACS antibodies were validated by the manufacturers. FMO (fluorescence minus one) was evaluated for every antibody to assess specificity of the stainings. Moreover, each antibody was in-house titrated to ensure optimal separation between positive and negative populations.

Immunostaining antibodies were validated by manufacturers and were used based in previous publications (Balemans, D. et al., Sci. Rep. 2017). As negative control, one section per slide was stained according to the same protocol excluding the primary antibody. This procedure was adopted for every staining used in the study.

Animals and other organisms

Policy information about studies involving animals; ARRIVE guidelines recommended for reporting animal research

Laboratory animals

Six- to seven-week-old wild type (WT) male BALB/c mice were purchased from Janvier. Six- to seven-week-old male Cpa3Cre/+ and WT male littermates on BALB/c background, generously provided by Prof. H.R. Rodewald, DKFZ, Heidelberg, Germany, were used to study the role of mast cells. Six- to ten-week-old female Igh7-/- (mice lacking IgE) on BALB/c background, generously provided by Prof. J. Strid, DKFZ, Imperial College London, were used to study the role of IgE, which were compared to WT female BALB/c mice. Six- to ten-week-old male Hrh1-/- KO mice on BALB/c background (Oriental Bioservice, INC, Kyoto, Japan) were used to study the role of the histamine 1 receptor. Mice were maintained under a 14h/10h dark/light cycle, at a temperature of 20-22 °C (45-70% humidity), provided with food and water ad libitum.

Wild animals

No wild animals were used in the study.

Field-collected samples

No field collected samples were used in the study.

Ethics oversight

All animal experiments were performed in accordance with the European Community Council or Canadian Council of Animal Care guidelines and approved by the Animal Care and Animal Experiments Committee of the Medical Faculty of the KU Leuven or Queen's University Animal Care Committee. There were no self-selection bias or other biases during subject recruitment.

Note that full information on the approval of the study protocol must also be provided in the manuscript.

Human research participants

Policy information about studies involving human research participants

Population characteristics

Food antigen injection: Eight healthy volunteers (HV, 8 female, 50 years, IQR [32-54]) free of abdominal symptoms, with no history of gastrointestinal disease, no previous gastrointestinal surgery or taking gastrointestinal medication, were recruited by public advertisement. Twelve IBS patients meeting the ROME III criteria (8 females, 29 years, IQR [21-39]) were recruited from the outpatient clinic of the University Hospitals Leuven. Allergy to soy, wheat, gluten and milk was excluded in all participants (anamnesis, skin-prick test and total IgE, tryptase and antigen-specific IgE in serum performed by a trained allergologist).
Trypsin-like-activity: 13 HV (10 females, 29 years IQR [23-47]) were recruited by public advertisement and were free of abdominal symptoms, had no gastrointestinal disease or surgery and were not on gastrointestinal medication. 48 IBS patients meeting the ROME III criteria (33 females, 31 years IQR [19-40]) were recruited from the outpatient clinic of the University Hospitals Leuven.

Bacterial identification in fecal samples: 64 HV (35 females, 49 years IQR [32-58]) were recruited by public advertisement and were free of abdominal symptoms, had no gastrointestinal disease or surgery and were not on gastrointestinal medication. 84 IBS patients meeting the ROME III criteria (66 females, 38 years IQR [25-50]) were recruited from the outpatient clinic of the University Hospitals Leuven.
Biopsy collection for immunofluorescence staining: 15 HV (13 females, 41 years IQR [32-52]) were recruited by public advertisement and were free of abdominal symptoms, had no gastrointestinal disease or surgery and were not on gastrointestinal medication. 22 IBS patients meeting the ROME III criteria (20 females, 31 years IQR [27-43]) were recruited from the outpatient clinic of the University Hospitals Leuven. All participants were invited to report their gastro-intestinal symptoms by means of an adapted version of the visual analogue scale (VAS) for IBS, assessing the intensity of their last episode of

	abdominal pain, abdominal discomfort and bloating (scored from 0 to 10).
Recruitment	As stated, healthy volunteers were recruited by public advertisement and IBS patients were recruited from the outpatient clinic of the University Hospitals Leuven. s. There were no self-selection bias or other biases during subject recruitment.
Ethics oversight	All experiments involving humans and human material were approved by the Medical Ethics Committee of the University Hospitals of Leuven and all patients provided informed consent (reference approval numbers: S51973, S55484 and S55485).

Note that full information on the approval of the study protocol must also be provided in the manuscript.

Flow Cytometry

Plots

Confirm that:

☒ The axis labels state the marker and fluorochrome used (e.g. CD4-FITC).

☒ The axis scales are clearly visible. Include numbers along axes only for bottom left plot of group (a 'group' is an analysis of identical markers).

☒ All plots are contour plots with outliers or pseudocolor plots.

☒ A numerical value for number of cells or percentage (with statistics) is provided.

Methodology

Sample preparation	Colon and small intestine were removed from mesenteric fat tissue, opened longitudinally and successively cleaned in cold phosphate-buffered saline (PBS) and Hank's Balanced Salt Solution (HBSS) (Gibco) supplemented with fetal calf serum (FCS, 1%, Lonza) and Penicillin/Streptomycin (Gibco) (100 µg/mL) (= wash medium). Epithelial cells were removed by an 8-minute incubation on a magnetic stirrer in warm (37°C) wash medium supplemented with DTT (1mM) and EDTA (1mM). After a washing step, tissue was cut in pieces smaller than 3mm and digested by a 25- to 30-min incubation on a magnetic stirrer in warm (37°C) MEM α containing Penicillin/Streptomycin (100 µg/mL), β-mercaptoethanol (50 µM, Sigma-Aldrich®), FCS (5%), Dnase (5U/mL, Roche), Collagenase V (0,85 mg/mL, Sigma-Aldrich®), Collagenase D (1,25 mg/mL, Roche), Dispase (1 mg/mL, Gibco). After digestion, cells were filtered through a 70 µm cell strainer and lamina propria cells were purified using a Percoll (VWR) gradient (44 to 67%). Purified cells were res re-suspended in PBS supplemented with fetal calf serum (1%) and Penicillin/Streptomycin (100 µg/mL) and counted prior to staining for Flow Cytometry.
Instrument	BD Canto HTS (BD Biosciences).
Software	FlowJo software (Tree Star Inc.).
Cell population abundance	The study did not involve sorted samples
Gating strategy	Single cell suspensions were labelled for flow cytometry analysis using fluorophore-conjugated anti-mouse antibodies for 30 min at 4°C using the antibodies listed in Extended Data Table 4. Living cells were identified using a viability dye (Fixable Viability Dye eFluor®450 or Fixable Viability Dye eFluor®506, eBioscience). For intracellular staining, cells were fixed for 30 minutes, washed and then permeabilized for 20 minutes using a Foxp3 / Transcription Factor Staining Buffer Set (eBioscience). Cells were incubated with intracellular antibodies for 1 hour at 4°C. Gating strategies are shown in Extended Data Fig. n and p, and Extended Data Fig. 4m. Neutrophils were gated for FSC/SSC, CD45 positive/alive, CD11b positive, Ly6G positive, SiglecF negative. Eosinophils were gated for FSC/SSC, CD45 positive/alive, CD11b positive, SiglecF positive. Mast cells were gated for FSC/SSC, CD45 positive/alive, CD117 positive FcεRI positive. T cells were gated for FSC/SSC, CD45 positive/alive, CD3 positive. CD4+ T cells were gated for FSC/SSC, CD45 positive/alive, CD3 positive, CD4 positive. Tregs were gated for FSC/SSC, CD45 positive/alive, CD3 positive, CD4 positive, FOXP3 positive. pTregs were gated for FSC/SSC, CD45 positive/alive, Helios negative, Nrp1 low, FOXP3 positive. Plasma cells were gated for FSC/SSC, CD45 positive/alive, CD19 positive, Ly6K positive. B cells were gated for FSC/SSC, CD45 positive/alive, IgM positive, B220 positive.

☒ Tick this box to confirm that a figure exemplifying the gating strategy is provided in the Supplementary Information.